doi:10.1093/brain/awu082 Brain 2014: 137; 1676–1700 | 1676

BRAIN
A JOURNAL OF NEUROLOGY

The wide spectrum of tubulinopathies: what are the key features for the diagnosis?

Nadia Bahi-Buisson,[1,2,3,4,5,*] Karine Poirier,[1,2,*] Franck Fourniol,[6,*] Yoann Saillour,[1,2] Stéphanie Valence,[1,2] Nicolas Lebrun,[1,2] Marie Hully,[5] Catherine Fallet Bianco,[7] Nathalie Boddaert,[8,9] Caroline Elie,[10] Karine Lascelles,[11] Isabelle Souville,[12] LIS-Tubulinopathies Consortium,[†] Cherif Beldjord[12] and Jamel Chelly[1,2]

1 Institut Cochin, Université Paris-Descartes, CNRS (UMR 8104), Paris, France
2 Inserm, U1016, Paris, France
3 Université Paris Descartes, Sorbonne Paris Cité, Institut Imagine, Paris, France
4 INSERM UMR-1163, Embryology and genetics of congenital malformations, Paris, France
5 Service de Neurologie pédiatrique, Assistance Publique-Hôpitaux de Paris (AP-HP), hôpital Necker, Paris, France
6 CRUK London Research Institute, London, UK
7 Université de Montreal–CHU Sainte Justine, Montreal (QC), Canada
8 Service de Radiologie Pédiatrique, AP-HP, hôpital Necker, Paris, France
9 Inserm, U797-INSERM-CEA, Service Hospitalier Frédéric Joliot, CEA, 4, place du General Leclerc, 91406, Orsay, France
10 BioInformatic Department-AP-HP, hôpital Necker-Enfants Malades, Paris, France
11 Evelina Children's Hospital, St Thomas Hospital, London, UK
12 Service de Biologie Moleculaire et Genetique, Pavillon Cassini AP-HP, Hôpital Cochin, Paris, France

*These authors contributed equally to this work.

[†]See Appendix 1.

Correspondence to: Nadia Bahi-Buisson, MD, PhD,
Paediatric Neurology Hopital Necker Enfants Malades,
Université Paris Descartes, APHP,
149 rue de Sevres 75015 Paris
E-mail: nadia.bahi-buisson@nck.aphp.fr

Complex cortical malformations associated with mutations in tubulin genes: *TUBA1A*, *TUBA8*, *TUBB2B*, *TUBB3*, *TUBB5* and *TUBG1* commonly referred to as tubulinopathies, are a heterogeneous group of conditions with a wide spectrum of clinical severity. Among the 106 patients selected as having complex cortical malformations, 45 were found to carry mutations in *TUBA1A* (42.5%), 18 in *TUBB2B* (16.9%), 11 in *TUBB3* (10.4%), three in *TUBB5* (2.8%), and three in *TUBG1* (2.8%). No mutations were identified in *TUBA8*. Systematic review of patients' neuroimaging and neuropathological data allowed us to distinguish at least five cortical malformation syndromes: (i) microlissencephaly ($n = 12$); (ii) lissencephaly ($n = 19$); (iii) central pachygyria and polymicrogyria-like cortical dysplasia ($n = 24$); (iv) generalized polymicrogyria-like cortical dysplasia ($n = 6$); and (v) a 'simplified' gyral pattern with area of focal polymicrogyria ($n = 19$). Dysmorphic basal ganglia are the hallmark of tubulinopathies (found in 75% of cases) and are present in 100% of central pachygyria and polymicrogyria-like cortical dysplasia and simplified gyral malformation syndromes. Tubulinopathies are also characterized by a high prevalence of corpus callosum agenesis (32/80; 40%), and mild to severe cerebellar hypoplasia and dysplasia (63/80; 78.7%). Foetal cases ($n = 25$) represent the severe end of the spectrum and show specific abnormalities that provide insights into the underlying pathophysiology. The overall complexity of tubulinopathies reflects the pleiotropic effects of tubulins and their specific spatio-temporal profiles of expression. In line with previous reports, this large cohort further clarifies overlapping phenotypes between tubuli-

Received October 18, 2013. Revised February 18, 2014. Accepted February 20, 2014

nopathies and although current structural data do not allow prediction of mutation-related phenotypes, within each mutated gene there is an associated predominant pattern of cortical dysgenesis allowing some phenotype–genotype correlation. The core phenotype of *TUBA1A* and *TUBG1* tubulinopathies are lissencephalies and microlissencephalies, whereas *TUBB2B* tubulinopathies show in the majority, centrally predominant polymicrogyria-like cortical dysplasia. By contrast, *TUBB3* and *TUBB5* mutations cause milder malformations with focal or multifocal polymicrogyria-like cortical dysplasia with abnormal and simplified gyral pattern.

Keywords: microlissencephaly; lissencephaly; polymicrogyria; microcephaly; pachygyria; tubulin

Introduction

The formation of the complex architecture of the mammalian brain requires a coordinated timing of proliferation, migration and layering, as well as differentiation of distinct neuronal populations. The cellular processes and related biological mechanisms underlying their disruption are traditionally used as a basis for the classification of the large spectrum of malformations of cortical development that represent a significant cause of neurological morbidity in children leading to intellectual disability, cerebral palsy, and/or epilepsy. This classification system divides brain malformations into disorders of (i) abnormal neuronal and glial proliferation; (ii) neuronal migration; and (iii) abnormal post-migrational development (Barkovich *et al.*, 2005, 2012).

The division of neuronal progenitors, as well as the striking morphology of neurons as they migrate and establish their dendritic and axonal arbors, implies a strictly regulated process of cytoskeletal structuring and polarization (Higginbotham and Gleeson, 2007; Hoogenraad and Bradke, 2009). Compelling evidence has demonstrated that the nervous system development is highly dependent upon the microtubule cytoskeleton. Microtubules are polymers of tubulin heterodimers, which are themselves assembled from various α- and β-tubulin isotypes encoded by separate genes (Lopata and Cleveland, 1987). Microtubule behaviour varies depending on isotype composition, suggesting that different isotypes may have distinct properties adapted to specific cellular functions (Joshi and Cleveland, 1990; Luduena, 1993).

Recent genetic studies have pointed out critical effects of tubulins and microtubule-associated proteins involvement in malformations of cortical development. Up to now mutations in tubulin genes encoding different α- and β-tubulin isotypes (*TUBA1A*, *TUBA8* and *TUBB2B*, *TUBB3*, *TUBB5*) and more recently γ-tubulin (*TUBG1*) have been shown to be involved in a large spectrum of developmental brain disorders (Keays *et al.*, 2007; Abdollahi *et al.*, 2009; Jaglin *et al.*, 2009; Tischfield *et al.*, 2010; Breuss *et al.*, 2012; Poirier *et al.*, 2013*a*). Mutations in *TUBA1A*, *TUBB2B*, *TUBB3* and *TUBB5* are heterozygous missense mutations whereas the unique *TUBA8* mutation consists of a homozygous 14 bp intronic deletion upstream of exon 2 (Keays *et al.*, 2007; Abdollahi *et al.*, 2009; Jaglin *et al.*, 2009; Tischfield *et al.*, 2010; Breuss *et al.*, 2012). All mutations in *TUBA1A* and *TUBB5* and *TUBB2B* are sporadic and occur *de novo* whereas *TUBB3* mutations are a mixture of familial and *de novo* mutations. The first tubulin gene involved in brain malformation encodes α-tubulin 1A. Initial reports highlighted the presence of specific abnormalities found in *TUBA1A*-related lissencephalies. These consist of a unique combination of microcephaly, variable cortical malformations that range from perisylvian pachygyria (also named, 'variant pachygyria' most prominent in posterior frontal, perisylvian and parietal regions) to posteriorly predominant lissencephalies associated with absence or hypoplasia of the anterior limb of the internal capsule, complete or partial agenesis of the corpus callosum and cerebellar and brain stem hypoplasia (Keays *et al.*, 2007; Poirier *et al.*, 2007; Bahi-Buisson *et al.*, 2008; Morris-Rosendahl *et al.*, 2008; Kumar *et al.*, 2010; Sohal *et al.*, 2012; Amrom *et al.*, 2013; Okumura *et al.*, 2013; Hikita *et al.*, 2014). Subsequently, the spectrum of *TUBA1A*-related lissencephaly was enlarged with the description of lissencephaly with cerebellar hypoplasia and 'simplified' gyral pattern plus complete corpus callosum agenesis and moderate cerebellar hypoplasia (Kumar *et al.*, 2010). More recently, *TUBA1A* mutations were also described in perisylvian asymmetrical polymicrogyria (Jansen *et al.*, 2011; Poirier *et al.*, 2013; Zanni *et al.*, 2013), and polymicrogyria-like cortical dysplasia (Cushion *et al.*, 2013). In parallel, five foetal cases that probably represent the more severe end of the spectrum of *TUBA1A* lissencephaly were reported, displaying a combination of complete to posteriorly predominant agyria, corpus callosum agenesis or hypogenesis, severe microcephaly, and variable brainstem and cerebellar defects, consistent with either the phenotype of classic lissencephaly or lissencephaly with cerebellar hypoplasia (Fallet-Bianco *et al.*, 2008; Lecourtois *et al.*, 2010).

Heterozygous missense *TUBB2B* mutations were initially described in patients with bilateral, asymmetric polymicrogyria, typically more predominant in the frontal and temporal lobes. Similar to *TUBA1A* mutations, *TUBB2B* mutation-related cortical dysgenesis was associated with dysmorphic basal ganglia, partial or complete agenesis of the corpus callosum and hypoplasia or dysplasia of the cerebellum (Jaglin *et al.*, 2009; Amrom *et al.*, 2013). Subsequently, *TUBB2B* mutations were described in symmetrical polymicrogyria as well as schizencephaly, further broadening the spectrum of *TUBB2B*-related cortical dysgenesis. Remarkably, in some cases the corpus callosum as well as the cerebellum were normal (Guerrini *et al.*, 2012; Romaniello *et al.*, 2012). Recently, Cushion *et al.* (2013) reported four additional severe cases of *TUBB2B* mutations showing in all cases polymicrogyria-like cortical dysplasia together with dysmorphic basal ganglia, brainstem and cerebellar vermian hypoplasia. Moreover, one of the *TUBB2B* mutated cases demonstrated a lissencephaly pattern with an agyric cortex, and bilateral band of heterotopic

cortex suggesting that an overlap may also exist in the *TUBA1A* and *TUBB2B* related lissencephalies (Cushion *et al.*, 2013).

TUBB3 mutations cause a more diffuse spectrum of brain malformations and neurological disabilities and certain phenotypes often segregate with particular amino acid substitutions (Poirier *et al.*, 2007; Tischfield *et al.*, 2010). Initially, heterozygous familial and *de novo TUBB3* missense mutations were reported in a paralytic eye movement disorder (i.e. congenital fibrosis of extraocular muscle, CFEOM3), which results from hypoplasia of the oculomotor nerve(s) combined with a sensorimotor polyneuropathy and mild to moderate intellectual disability, depending upon the specific amino acid substitution. Brain malformations include agenesis or hypoplasia of commissural axon tracts, hypoplasia of the corticospinal tract, and dysmorphic basal ganglia with fusion of the caudate and putamen (Tischfield *et al.*, 2010). Subsequently, the *TUBB3* phenotypic spectrum was enlarged with frontal polymicrogyria or simplified and disorganized gyral patterning, brainstem and cerebellar vermian hypoplasia and basal ganglia dysmorphism. Also, one foetal case was reported with microlissencephaly and corpus callosum agenesis, severe brainstem and cerebellar hypoplasia and dysmorphic basal ganglia (Poirier *et al.*, 2010).

More recently, recurrent p.E410K TUBB3 mutations were described, resulting in a specific clinical association that combines intellectual disability, Kallmann syndrome, congenital fibrosis of extraocular muscles, facial weakness, tracheomalacia, vocal cord paralysis and later-onset cyclic vomiting and progressive peripheral neuropathy. Patients show on MRI, no cortical malformations but a thin corpus callosum and anterior commissures, as well as hypoplastic to absent olfactory bulbs, oculomotor and facial nerves, which are consistent with abnormalities in axon guidance and maintenance. This peculiar association led the authors to define it as the 'TUBB3 E410K syndrome' (Chew *et al.*, 2013).

Subsequently, *TUBB5* mutations were reported in three patients displaying various patterns of brain dysgenesis ranging from gyral simplification to focal polymicrogyria and microcephaly (Breuss *et al.*, 2012). Far less common is the homozygous deletion in *TUBA8* that was reported in two consanguineous pedigrees with polymicrogyria and corpus callosum hypoplasia in association with optic nerve hypoplasia (Abdollahi *et al.*, 2009). However, although this phenotype merges with other tubulinopathies, additional mutations are needed to definitively support *TUBA8* as a polymicrogyria-associated gene. Finally, most recently the tubulin *TUBG1*, a gamma tubulin involved in centrosome organization, was also found to be mutated in three patients with lissencephaly with microcephaly (Poirier *et al.*, 2013*a*).

In the present paper, we report the largest cohort of 80 tubulin-related cortical malformations that result from tubulin mutations in *TUBA1A*, *TUBB2B*, *TUBB3*, *TUBB5*, or *TUBG1* genes. We have attempted to refine the spectrum of cortical dysgenesis in our cohort and identified five distinct malformation subtypes that correspond to agyria-pachygyria (lissencephaly), microlissencephaly, 'central' pachygyria and polymicrogyria-like cortical dysplasia, generalized polymicrogyria-like cortical dysplasia, and finally a 'simplified' gyral pattern with area of focal polymicrogyria. Findings on all foetal cases are reported in detail elsewhere (Fallet-Bianco *et al.* submitted for publication). Based on structural data, we discuss the phenotype according to the position of mutated residues and putative consequences of mutations on tubulin assembly and interactions. With five tubulin genes involved, together with previous published cases, the aim of this paper is to propose a diagnostic strategy and to identify genotype–phenotype correlations to further improve molecular testing and diagnosis of malformations of cortical development.

Patients and methods

Patient selection

As part of our increasing collection of patients with malformations of cortical development, comprising to date 540 living patients and 60 foetuses (corresponding to 564 sporadic cases and 36 familial cases) referred to our laboratory for genetic and molecular investigations, we identified mutations in tubulin genes for 80 patients with cortical malformations. Unexplained cases of malformations of cortical development referred in our laboratory for molecular screening encompass the whole range of non-syndromic cortical dysgenesis, agyria-pachygyria ($n = 58$), typical polymicrogyria ($n = 420$) or polymicrogyria-like cortical dysplasia ($n = 60$) or gyral simplification pattern ($n = 62$).

Of these, 106 patients met the criteria of complex cortical malformation, i.e. combination of cortical dysgenesis, either agyria-pachygyria ($n = 23$), microlissencephaly ($n = 16$), polymicrogyria or polymicrogyria-like cortical dysplasia ($n = 42$), or 'simplified' gyral pattern with area of focal polymicrogyria ($n = 25$) plus partial or complete agenesis of corpus callosum, dysmorphic basal ganglia, brainstem hypoplasia and/or cerebellar hypoplasia or dysplasia and/or microcephaly. All were sporadic cases except for six familial cases from three families. Included patients were from 20 centres in France and Switzerland. All patients were known personally to at least one of the authors. Eighty of 600 (13.3%) patients with tubulinopathies were identified. Of these 80 patients (55 living patients and 25 foetuses), 39 were previously reported by our group and re-evaluated for the purpose of this review, 18 patients with *TUBA1A* mutations, five patients with *TUBB2B* mutations, 10 patients with *TUBB3* mutations, three with *TUBB5* mutations and three with *TUBG1* mutations (Keays *et al.*, 2007; Poirier *et al.*, 2007, 2010, 2013*a*, *b*; Fallet-Bianco *et al.*, 2008; Jaglin and Chelly, 2009; Lecourtois *et al.*, 2010; Breuss *et al.*, 2012).

Mutation analysis

Blood samples for DNA preparation and genetic investigations were obtained with informed consent from parents and/or patients. DNA was extracted using standard protocols. For each patient, array-CGH was normal and *LIS1*, *DCX* and *GPR56* mutations and deletions were excluded. Mutation analysis of the coding regions of these six genes (*TUBA1A*, *TUBA8*, *TUBB2B*, *TUBB3* and *TUBB5* or *TUBG1)*, was carried out on all patients, as described previously (Keays *et al.*, 2007; Abdollahi *et al.*, 2009; Jaglin and Chelly, 2009; Poirier *et al.*, 2010, 2013*a*, *b*; Breuss *et al.*, 2012), and sequences of primers and PCR conditions are available upon request. For each patient, the mutation was tested by direct sequencing in both parents' DNA to assess

whether they occurred *de novo*, or were inherited from one of the parents.

Clinical information, brain magnetic resonance imaging and classification

All patients are followed regularly in various departments of Paediatric Neurology and were known personally to at least one of the authors and were re-examined for the purpose of the study. Both the clinical information and brain MRIs were obtained and centralized by N.B.B. at the Paediatric Neurology unit of Necker Enfants Malades Hospital, Paris Descartes University. Detailed information regarding family history, pre- and perinatal events, motor development, cognitive function, neurological examination including head circumference and ophthalmological features was recorded. With regards to the epilepsy, age of seizure onset, main seizure type and response to antiepileptic drugs was determined.

Brain MRIs were reviewed by at least two investigators (N.B.B and N.B) for the purpose of classifying patients. The scans were reviewed using a proforma in which the following abnormalities (using widely accepted criteria) were recorded. Cortical malformations were classified as follows: polymicrogyria was diagnosed according to the three recognized criteria (Leventer *et al.*, 2010): (i) irregular surface of cortex; (ii) thickened or overfolded cortex aspect; and (iii) irregularity at the grey–white interface. However, as a large proportion of patients did not show all the criteria of typical polymicrogyria, we classified this as atypical polymicrogyria or polymicrogyria-like cortical dysplasia (Cushion *et al.*, 2013). Polymicrogyria and polymicrogyria-like cortical dysplasia were further classified according to the pattern, distribution and topography of the abnormality. Where no specific pattern was identified, they were classified as focal (in association with irregular sulcal pattern but no clear topographic distribution) or multifocal (patchy in both hemispheres without any particular pattern or gradient). Lissencephaly was classified according to the severity (agyria to pachygyria and subcortical band heterotopia) and the maximal location (fronto-parietal i.e. anteriorly predominant and parieto-occipital or central i.e. posteriorly predominant) as described by Dobyns *et al*. (1999). Microlissencephaly was first reported by Norman *et al.* (1976) in a patient combining thick and lissencephalic cortex and severe microcephaly. Barkovich *et al.* (2012) defines microlissencephaly as congenital microcephaly with thick or relatively thick cortex. Here, microlissencephaly refers to severe microcephaly with biometric brain parameters below the third percentile without intrauterine growth retardation and lissencephaly with hemispheric surface completely smooth lacking primary fissures and olfactory sulci.

After this initial classification, the posterior fossa was reviewed with particular attention to the brainstem, the cerebellar vermis and the cerebellar hemispheres. In each case, 'hypoplasia' refers to small size but normal anatomy whereas 'dysplasia' refers to abnormal foliation or disorientation of fissures. Abnormalities of the corpus callosum were categorized as follows: agenesis (absence of the entire corpus callosum), hypogenesis (absence of the rostrum with small or absent splenium and small or absent inferior genu); hypoplasia (all parts formed but decreased thickness) or dysmorphic (abnormal shape of any part of the corpus callosum). Basal ganglia abnormalities were defined as either hypertrophy of the striatum or thalamus (when the volume is increased based on a consensus from both investigators), or dysmorphy with fusion between caudate and putamen (when the anterior horn of the internal capsule is not visible).

Results

Genotype–phenotype analysis

In this study, *TUBA1A*, *TUBB2B*, *TUBB3*, *TUBB5* or *TUBG1* mutations were identified in 74 sporadic patients with diffuse cortical malformations (13.1% of sporadic cases) and six familial cases with dominant segregation of the disorders (three families) (16.6% of familial cases). Details concerning distribution of these mutations and associated phenotypes are provided in Fig. 1 and Table 1. Briefly, 45 *de novo TUBA1A* missense mutations were identified in 27 sporadic living patients and 18 foetuses with malformations of cortical development. Of these, 17 are described here for the first time. Three hot spots were found, the most frequent being missense mutations affecting Arg264 (seven patients and one foetus), Arg402 (resulting in p.R402H in five patients and p.R402C in two patients) and Arg422 (resulting in p.R422H in two patients and p.R422C in one patient). These hot spot mutations represent 40% of all known *TUBA1A* mutations. Eighteen *de novo TUBB2B* missense mutations were identified in 12 sporadic living patients and six foetuses with cortical malformations. Among these mutations, 12 are novel and three recurrent mutations p.I202T, p.S172P and p.F265L were found in two patients, respectively. Eight *TUBB3* missense mutations, including a novel one, were found in five sporadic patients and three families. One recurrent mutation, p.E205K was found in one family and one sporadic patient. The three patients with *TUBB5* mutations and the three patients with *TUBG1* mutations have been previously reported but were revisited for the purpose of the study. No mutation was found in the *TUBA8* gene (Table 1 and Fig. 1).

Looking back at their brain MRIs we identified five major subtypes of malformations detailed below: microlissencephaly in 12 patients, agyria-pachygyria (lissencephaly) in 19, central pachygyria and polymicrogyria-like cortical dysplasia in 24, diffuse polymicrogyria-like cortical dysplasia in six, and finally a 'simplified' gyral pattern with area of focal polymicrogyria in 19. Clinical and brain imaging features are summarized in Table 1. Representative MRI images are shown in Figs 2–8.

Microlissencephaly

This pattern of severe microcephaly without intrauterine growth retardation and lissencephaly with hemispheres lacking primary fissures and olfactory sulci represents the most severe end of the spectrum of tubulinopathies. It is identified exclusively in foetal cases (eight males, four females). All foetuses had a neuropathological examination—two previously reported (Lecourtois *et al.*, 2010; Poirier *et al.*, 2010). In all cases, the pregnancy was terminated for medical reasons at median gestation of 25 weeks (range 16–36) after a prenatal diagnosis of microcephaly, corpus callosum agenesis and severe brain dysgenesis.

In all cases, brain MRI demonstrated an absent to poorly operculized cortex and virtually no visible gyration together with severe

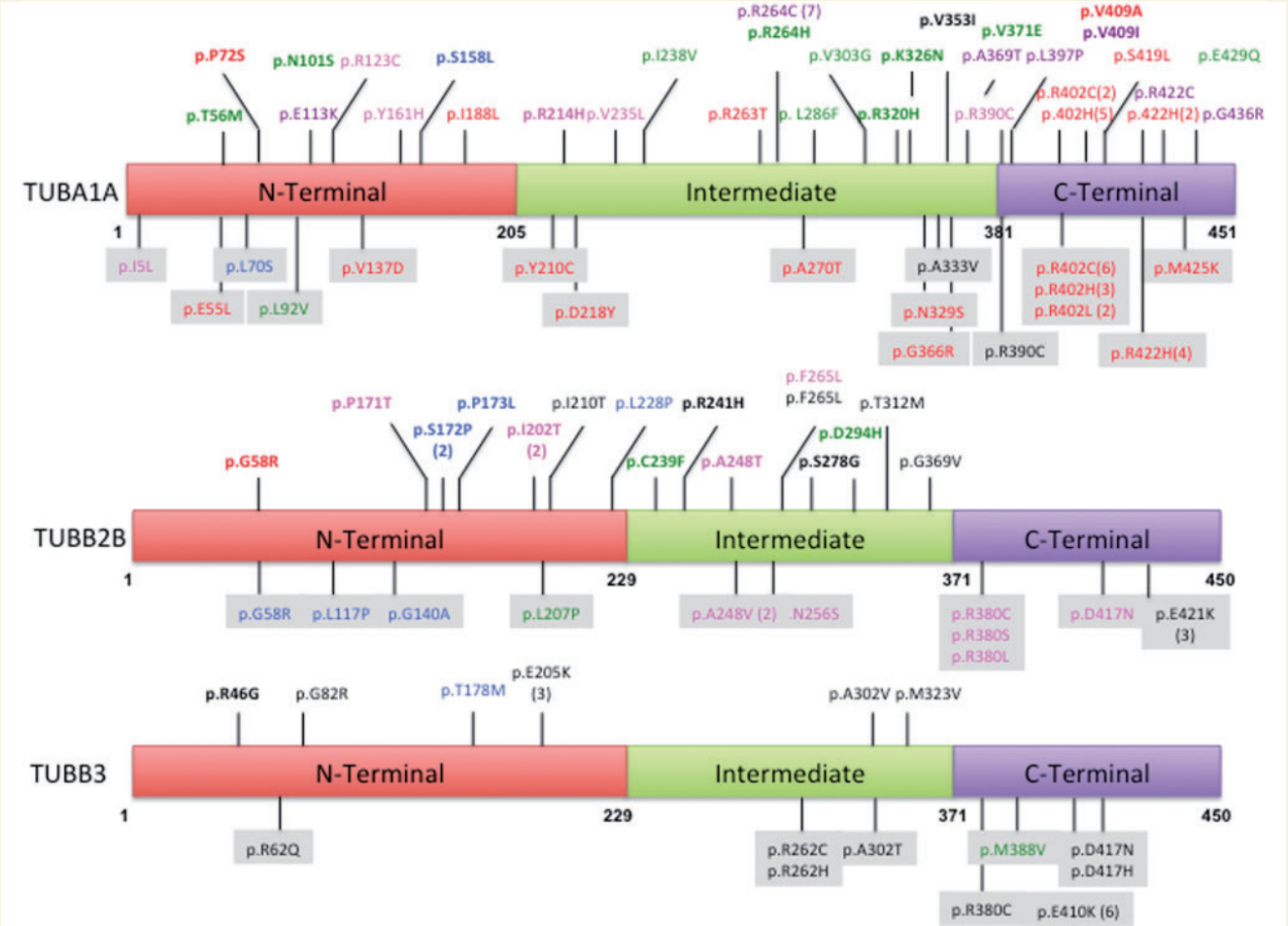

Figure 1 Schematic representations of the functional domains of TUBA1A, TUBB2B and TUBB3 tubulin subunits and distribution of mutations associated with malformations of cortical development. Illustrated domains are the N-terminal that contains the guanine nucleotide-binding region, intermediate domain, and C-terminal domains that constitute the binding surface for microtubule-associated proteins and molecular motors such as kinesins and dyneins. In β-tubulin, they correspond to residues 1–229, 230–371, and 372–450, (Lowe *et al.*, 2001) and in α-tubulin, to residues 1–205, 206–381, 382–451 (Nogales *et al.*, 1998), respectively. Mutations associated with a lissencephaly (classic and with cerebellar hypoplasia) phenotype are indicated in red, with microlissencephaly in green, with central pachygyria in purple, central polymicrogyria-like cortical dysplasia in pink with generalized polymicrogyria-like cortical dysplasia in blue, with multifocal polymicrogyria and simplified gyral pattern in black. Grey markers indicate the distribution of the other reported TUBA1A, TUBB2B and TUBB3 mutations. For recurrent variations the number of occurrences is indicated in brackets.

cerebellar hypoplasia and complete (10/12; 83.3%) or partial (2/12; 16.7%) agenesis of the corpus callosum. In this subtype, the basal ganglia were either not visible, virtually absent (5/11; 45.5%) or severely hypoplastic (6/11; 54.5%). Associated malformations included a very thin brainstem with flattening of the pons in all cases.

In patients with microlissencephaly, tubulin mutations included mainly the *TUBA1A* gene (p.T56M, p.N101S, p.R264H, p.L286F, p.V303G, p.R320H, p.K326N, p.V371E, and p.E429Q), but also *TUBB2B* (p.D249H, p.C239F) and *TUBB3* (p.M388V) in one case. None of these mutations have been found in other tubulinopathies to date. More interestingly, they represent the first dominant aetiology of microlissencephaly, as other known genetic causes, including mutations in *NDE1* or *WDR62*, are of autosomal recessive inheritance (Bilguvar *et al.*, 2010).

Lissencephaly

This pattern was found in 11 living patients and eight foetuses (11 males, eight females). Six out of eight foetuses had a neuropathological examination—three previously reported (Fallet-Bianco *et al.*, 2008), whereas in the remaining two the diagnosis was made on foetal MRI as foetopathological analysis was declined by the parents. In all cases, the pregnancy was terminated for medical reasons at a mean of 30.7 weeks gestation after a prenatal diagnosis of severe brain dysgenesis on ultrasound and MRI.

Table 1 Overview of MRI characteristics in patients with tubulinopathies

Case ID	Gene	Gender	Nucleotidic sequence variation	Proteic sequence variation	Inheritance	Cortical dysgenesis (diagnosis group assignment)	Corpus callosum	Cerebellum	Age or TOP	Head size (SD)	Tubulin mutations group/structural prediction	Reference
LIS_TUB_005_foetus01	*TUBA1A*	M	**c.959G > A**	**p.R320H**	*De novo*	MicroLIS	p.ACC	Sev_Ver_HS_Dys	25 GW		B	This series
LIS_TUB_006_fœtus03	*TUBA1A*	F	c.908T > G	p.V303G	*De novo*	MicroLIS	p.ACC	Sev_Ver_HS_Dys	36 GW		E	Lecourtois *et al.*, 2010
LIS_TUB_007_fœtus04	*TUBA1A*	M	c.856C > T	p.L286F	*De novo*	MicroLIS	c.ACC	Mod_Ver_Hypo	23 GW		C	Fallet-Bianco *et al.*, 2008
LIS_TUB_004_fœtus08	*TUBA1A*	M	**c.978A > C**	**p.K326N**	*De novo*	MicroLIS	c.ACC	Sev_Ver_HS_Dys	23 GW		B	This series
LIS_TUB_001_fœtus09	*TUBA1A*	F	**c.1285G > C**	**p.E429Q**	*De novo*	MicroLIS	c.ACC	Sev_Ver_Hypo	25 GW		D	This series
LIS_TUB_008_ fœtus13	*TUBB2B*	M	**c.716G > T**	**p.C239F**	*De novo*	MicroLIS	c.ACC	Sev_Ver_HS_Dys	16 GW		E	This series
LIS_TUB_010_ fœtus17	*TUBB3*	M	c.1162A > G	p.M388V	*De novo*	MicroLIS	c.ACC	Sev_Ver_Hypo	27 GW		E	Poirier *et al.*, 2010
LIS_TUB_003_ fœtus18	*TUBA1A*	M	**c.167C > T**	**p.T56M**	*De novo*	MicroLIS	c.ACC	Sev_Ver_Hypo	24.3 GW		C	This series
LIS_TUB_009_ fœtus19	*TUBB2B*	M	**c.745G > C**	**p.D249H**	*De novo*	MicroLIS	c.ACC	Sev_Ver_Hypo	27 GW		C	This series
LIS_TUB_002_ fœtus20	*TUBA1A*	F	**c.790C > T**	**p.R264H**	*De novo*	MicroLIS	c.ACC	Sev_Ver_Hypo	24 GW		D	This series
LIS_TUB_080_ fœtus24	*TUBA1A*	F	**c.1112T > A**	**p.V371E**	*De novo*	MicroLIS	c.ACC	Sev_Ver_Hypo	23.3 GW		C	This series
LIS_TUB_079_ fœtus25	*TUBA1A*	M	**c.302A > G**	**p.N101S**	*De novo*	MicroLIS	c.ACC	Sev_Ver_HS_Dys	25 GW		A	This series
LIS_TUB_017 fœtus02	*TUBA1A*	M	**c.1205G > A**	**p.R402H**	*De novo*	LIS_sev_Agyria	c.ACC	Mild_Ver_Hypo	29 GW		D	This series
LIS_TUB_022_ fœtus05	*TUBA1A*	M	c.712A > G	p.I238V	*De novo*	LIS_sev_Agyria	c.ACC	Mod_Ver_Hypo	25 GW		B	Fallet-Bianco *et al.*, 2008
LIS_TUB_025 fœtus06	*TUBA1A*	M	c.787C > A	p.P263T	*De novo*	LCH_sev	c.ACC	Sev_Ver_Hypo	26 GW		D	Fallet-Bianco *et al.*, 2008
LIS_TUB_021_ fœtus07	*TUBA1A*	M	c.1204C > T	p.R402C	*De novo*	LIS_sev_Agyria	dysmCC_HypoCC	Mild_Ver_Hypo	35 GW		D	Fallet-Bianco *et al.*, 2008
LIS_TUB_018_ fœtus10	*TUBA1A*	F	**c.1265G > A**	**p.R422H**	*De novo*	LIS_sev_Agyria	c.ACC	Mild_Ver_Hypo	28 GW		D	This series
LIS_TUB_013_ fœtus14	*TUBB2B*	F	**c.302G > A**	**p.G98R**	*De novo*	LIS_sev_Agyria	c.ACC	Normal	32.8 GW		E	This series
LIS_TUB_012_ fœtus22	*TUBA1A*	F	**c.214 C > T**	**p.P72S**	*De novo*	LIS_sev_Agyria	dysmCC_HypoCC	Sev_Ver_Hypo	37.8 GW		E	This series
LIS_TUB_011_ fœtus23	*TUBA1A*	M	**c.1226T > C**	**p.V409A**	*De novo*	LCH_sev	c.ACC	Sev_Ver_Hypo	32 GW		D	This series
LIS_TUB_014	*TUBA1A*	M	**c.1205G > A**	**p.R402H**	*De novo*	LIS_sev_Agyria	hypogeneticCC	Sev_HS_Dys	4 y	−4	D	This series
LIS_TUB_015	*TUBA1A*	M	**c.1205G > A**	**p.R402H**	*De novo*	LIS_sev_Agyria	hypogeneticCC	Sev_HS_Dys	1 y	−4	D	This series
LIS_TUB_016	*TUBA1A*	F	**c.1205G > A**	**p.R402H**	*De novo*	LIS_sev_Agyria	hypogeneticCC	Ver_Dys	1.5 y	−3	D	This series
LIS_TUB_019	*TUBA1A*	M	**c.1204C > T**	**p.R402C**	*De novo*	LIS_mod	dysmCC_HypoCC	Mild_Ver_Hypo	10 y	−3	D	This series
LIS_TUB_020	*TUBA1A*	F	c.1265G > A	p.R422H	*De novo*	LIS_mod	dysmCC_HypoCC	Mild_Ver_Dys	7 y	−4	D	Bahi-Buisson *et al.*, 2008
LIS_TUB_023	*TUBA1A*	M	c.1205G > A	p.R402H	*De novo*	LIS_sev_Agyria	hypogeneticCC	Sev_HS_Dys	12 y	−3	D	Keays *et al.*, 2007; Poirier *et al.*, 2007; Bahi-Buisson *et al.*, 2008

(continued)

Table 1 Continued

Case ID	Gene	Gender	Nucleotidic sequence variation	Proteic sequence variation	Inheritance	Cortical dysgenesis (diagnosis group assignment)	Corpus callosum	Cerebellum	Age or TOP	Head size (SD)	Tubulin mutations group/structural prediction	Reference
LIS_TUB_024	*TUBA1A*	M	c.1256C > T	p.S419L	*De novo*	LIS_mod	hypogeneticCC	Normal	18 y	−1	D	Poirier *et al.*, 2007; Bahi-Buisson *et al.*, 2008
LIS_TUB_026	*TUBA1A*	F	c.562 A > C	p.I188L	*De novo*	LCH_mod_SBH	p.ACC	Sev_Ver_Hypo	2.5 y	−4	E	Poirier *et al.*, 2007; Bahi-Buisson *et al.*, 2008
LIS_TUB_027	*TUBG1*	F	c.991A > C	p.T331P	*De novo*	LIS_mod_SBH	dysmCC_HypoCC	Normal	31 y	−1		Poirier *et al.*, 2013*a*
LIS_TUB_028	*TUBG1*	F	c.1160T > C	p.L387P	*De novo*	LIS_sev_Agyria	dysmCC_HypoCC	Normal	21 y	−5.5		Poirier *et al.*, 2013*a*
LIS_TUB_029	*TUBG1*	M	c.275A > G	p.Y92C	*De novo*	LIS_sev_Agyria	dysmCC_HypoCC	Normal	1.5 y	−4		Poirier *et al.*, 2013*a*
LIS_TUB_043_foetus11	*TUBA1A*	M	**c.641G > A**	**p.R214H**	*De novo*	Central_PMG	c.ACC	Normal	23 GW		B	This series
LIS_TUB_048_foetus16	*TUBB2B*	M	**c.742G > A**	**p.A248T**	*De novo*	Central_PMG	Normal	Mild_Ver_Hypo	28.5 GW		E	This series
LIS_TUB_030	*TUBA1A*	M	**c.1105G > A**	**p.A369T**	*De novo*	Central_Pachy	dysmCC_HypoCC	Mild_Ver_Hypo	11 y	−2	C	This series
LIS_TUB_031	*TUBA1A*	M	**c.337G > A**	**p.E113K**	*De novo*	Central_Pachy	Normal	Normal	11 y	−3	D	This series
LIS_TUB_032	*TUBA1A*	M	**c.1225G > A**	**p.V409I**	*De novo*	Central_Pachy	dysmCC_HypoCC	Normal	10 y	−2	D	This series
LIS_TUB_033	*TUBA1A*	F	**c.790C > T**	**p.R264C**	*De novo*	Central_Pachy	Normal	Mild_Ver_Hypo	1.5 y	−5	D	This series
LIS_TUB_034	*TUBA1A*	F	**c.790C > T**	**p.R264C**	*De novo*	Central_Pachy	hypogeneticCC	Normal	6.5 y	−4	D	This series
LIS_TUB_035	*TUBA1A*	M	**c.790C > T**	**p.R264C**	*De novo*	Central_Pachy	Normal	Mild_Ver_Hypo	6 y	−3	D	This series
LIS_TUB_036	*TUBA1A*	M	c.790C > T	p.R264C	*De novo*	Central_Pachy	Normal	Mild_Ver_Hypo	2 y	−4.5	D	Poirier *et al.*, 2007; Bahi-Buisson *et al.*, 2008
LIS_TUB_037	*TUBA1A*	M	c.790C > T	p.R264C	*De novo*	Central_Pachy	hypogeneticCC	Mild_Ver_Dys	4.5 y	−4	D	Poirier *et al.*, 2007; Bahi-Buisson *et al.*, 2008
LIS_TUB_038	*TUBA1A*	M	c.1306G > T	p.G436R	*De novo*	Central_Pachy	dysmCC_HypoCC	Normal	7 y	−3	D	Bahi-Buisson *et al.*, 2008
LIS_TUB_039	*TUBA1A*	M	c.1190T > C	p.L397P	*De novo*	Central_Pachy	hypogeneticCC	Normal	5.5 y	−4	D	Bahi-Buisson *et al.*, 2008
LIS_TUB_040	*TUBA1A*	M	c.790C > T	p.R264C	*De novo*	Central_Pachy	Normal	Mild_Ver_Hypo	1.5 y	−4	D	Bahi-Buisson *et al.*, 2008
LIS_TUB_041	*TUBA1A*	M	c.790C > T	p.R264C	*De novo*	Central_Pachy	p.ACC	Normal	7 y	−4	D	Bahi-Buisson *et al.*, 2008
LIS_TUB_042	*TUBA1A*	F	c.1264C > T	p.R422C	*De novo*	Central_Pachy	dysmCC_HypoCC	Mild_Ver_Dys	4.5 y	−3	D	Bahi-Buisson *et al.*, 2008
LIS_TUB_044	*TUBA1A*	F	**c.367C > T**	**p.R123C**	*De novo*	Central_PMG	Normal	Ver_Dys	3 y	−3	C	This series

(continued)

Table 1 Continued

Case ID	Gene	Gender	Nucleotidic sequence variation	Proteic sequence variation	Inheritance	Cortical dysgenesis (diagnosis group assignment)	Corpus callosum	Cerebellum	Age or TOP	Head size (SD)	Tubulin mutations group/structural prediction	Reference
LIS_TUB_045	*TUBA1A*	M	c.1168C > T	p.R390C	*De novo*	Central_PMG	dysmCC_HypoCC	Ver_Dys	1 y	−3	D	Poirier *et al.*, 2013*b*
LIS_TUB_046	*TUBA1A*	M	c.703 G > T	p.V235L	*De novo*	Central_PMG	dysmCC_HypoCC	Normal	7.5 y	1	B	Poirier *et al.*, 2013*b*
LIS_TUB_047	*TUBA1A*	F	c.481 T > C	p.Y161H	*De novo*	Central_PMG	dysmCC_HypoCC	Ver_Dys	11 y	− 3	C	Poirier *et al.*, 2013*b*
LIS_TUB_049	*TUBB2B*	F	**c.605T > C**	**p.I202T**	*De novo*	Central_PMG	hypogeneticCC	Mild_Ver_Hypo	10 y	−2	E	This series
LIS_TUB_050	*TUBB2B*	M	**c.605T > C**	**p.I202T**	*De novo*	Central_PMG	hypogeneticCC	Mild_Ver_Hypo	15 y	0	E	This series
LIS_TUB_051	*TUBB2B*	M	**c.511C > A**	**p.P171T**	*De novo*	Central_PMG	p.ACC	Sev_Ver_Dys	17 y	−1	A	This series
LIS_TUB_052	*TUBB2B*	F	c.793T > C	p.F265L	*De novo*	Central_PMG	dysmCC_HypoCC	Sev_Ver_Dys	1.5 y	−3	E	This series
LIS_TUB_078	*TUBA1A*	F	**c.1186G > T**	**p.D396Y**	*De novo*	Central_PMG	p.ACC	Sev_Ver_Dys	4 y	−3	D	This series
LIS_TUB_056_foetus12	*TUBB2B*	M	c.514T > C	p.S172P	*De novo*	Generalized PMG	c.ACC	Mild_Ver_Hypo	27 GW		A	Jaglin *et al.*, 2009
LIS_TUB_054_foetus15	*TUBB2B*	M	c.518C > T	p.P173L	*De novo*	Generalized PMG	c.ACC	Mild_Ver_Hypo	25 GW		E	This series
LIS_TUB_053_foetus21	*TUBA1A*	F	**c.473C > T**	**p.S158L**	*De novo*	Generalized PMG	c.ACC	Sev_Ver_HS_Dys	24.5 GW		E	This series
LIS_TUB_055	*TUBB2B*	M	c.514T > C	p.S172P	*De novo*	Generalized PMG	c.ACC	Sev_Ver_HS_Dys	3 y	− 5	A	This series
LIS_TUB_057	*TUBB2B*	M	c.683T > C	p.L228P	*De novo*	Generalized PMG	c.ACC	Sev_Ver_HS_Dys	1 y	−5	E	Jaglin *et al.*, 2009
LIS_TUB_058	*TUBB3*	F	c.533C > T	p.T178M	*De novo*	Generalized PMG	c.ACC	Sev_Ver_HS_Dys	5 y	−4	A	Poirier *et al.*, 2010
LIS_TUB_059	*TUBA1A*	M	**c.1057G > A**	**p.V353I**	*De novo*	Simp_Gyr	p.ACC	Normal	4 y	−2	E	This series
LIS_TUB_060	*TUBB2B*	M	**c.1106G > T**	**p.G369V**	*De novo*	PMG_multi	hypogeneticCC	Ver_Dys	9 y	−1	E	This series
LIS_TUB_061	*TUBB2B*	F	**c.722G > A**	**p.R241H**	*De novo*	Simp_Gyr	Normal	Normal	12 y	−1	B	This series
LIS_TUB_062	*TUBB2B*	F	**c.832A > G**	**p.S278G**	*De novo*	Simp_Gyr	hypogeneticCC	Sev_Ver_Dys	0.9 y	−2.5	C	This series
LIS_TUB_063	*TUBB3*	F	**c.136C > G**	**p.R46G**	*De novo*	PMG_multi	dysmCC_HypoCC	Ver_Dys	2 y	−3	B	This series
LIS_TUB_064	*TUBB2B*	M	c.793C > T	p.F265L	*De novo*	PMG_multi	dysmCC_HypoCC	Sev_HS_Dys	36 y	−4	E	Jaglin *et al.*, 2009
LIS_TUB_065	*TUBB2B*	M	c.629T > C	p.I210T	*De novo*	PMG_multi	hypogeneticCC	Sev_HS_Dys	13 y	−4	E	Jaglin *et al.*, 2009
LIS_TUB_066	*TUBB2B*	M	c.935C > T	p.T312M	*De novo*	PMG_multi	dysmCC_HypoCC	Ver_Dys	5 y	−2	E	Jaglin *et al.*, 2009
LIS_TUB_067	*TUBB3*	M	c.633G > A	p.E205K	*De novo*	PMG_multi	dysmCC_HypoCC	Ver_Dys	8 y	−2	E	Poirier *et al.*, 2010
LIS_TUB_068	*TUBB3*	F	c.905C > T	p.A302V	*Inherited*	Simp_Gyr	hypogeneticCC	Ver_Dys	3 y	−2	E	Poirier *et al.*, 2010
LIS_TUB_069	*TUBB3*	M	c.633G > A	p.E205K	*Inherited*	PMG_multi	dysmCC_HypoCC	Ver_Dys	9 y	−1	E	Poirier *et al.*, 2010
LIS_TUB_070	*TUBB3*	F	c.905C > T	p.A302V	*Inherited*	Simp_Gyr	hypogeneticCC	Ver_Dys	40 y	−1	E	Poirier *et al.*, 2010

(continued)

Table 1 Continued

Case ID	Gene	Gender	Nucleotidic sequence variation	Proteic sequence variation	Inheritance	Cortical dysgenesis (diagnosis group assignment)	Corpus callosum	Cerebellum	Age or TOP	Head size (SD)	Tubulin mutations group/structural prediction	Reference
LIS_TUB_071	*TUBB3*	M	c.967A > G	p.M323V	*Inherited*	Simp_Gyr	hypogeneticCC	Ver_Dys	4 y	−0.5	B	Poirier *et al.*, 2010
LIS_TUB_072	*TUBB3*	F	c.633G > A	p.E205K	*Inherited*	PMG_multi	dysmCC_HypoCC	Ver_Dys	10 y	−0.5	E	Poirier *et al.*, 2010
LIS_TUB_073	*TUBB3*	M	c.244G > A	p.G82R	*De novo*	PMG_multi	p.ACC	Ver_Dys	5 y	0	E	Poirier *et al.*, 2010
LIS_TUB_074	*TUBB3*	M	c.967A > G	p.M323V	*Inherited*	Simp_Gyr	hypogeneticCC	Ver_Dys	38 y	0	B	Poirier *et al.*, 2010
LIS_TUB_075	*TUBB5*	F	c.1201G > A	p.E401K	*De novo*	Simp_Gyr	p.ACC	Normal	3 y	−4		Breuss *et al.*, 2012
LIS_TUB_076	*TUBB5*	M	c.1057G > A	p.V353I	*De novo*	Simp_Gyr	dysmCC_HypoCC	Normal	4.8 y	−4		Breuss *et al.*, 2012
LIS_TUB_077	*TUBB5*	M	c.895A > G	p.M299V	*De novo*	PMG_multi	hypogeneticCC	Ver_Dys	3 y	−2		Breuss *et al.*, 2012

In bold are the mutations newly described here.
M = males; F = females; y = years; GW = gestation weeks; TOP = termination of pregnancy; CC = corpus callosum; c.ACC = complete corpus callosum agenesis; p.ACC = partial corpus callosum agenesis; mod = moderate; sev = severe; Ver = vermian; Hypo = hypoplasia; Dys = dysplasia; dysm = dysmorphic; N/A = not available; N = normal. Head size is presented in SD (standard deviation).
Diagnosis group assignment allowed us to define five subgroups: (i) MicroLIS = microlissencephaly; (ii) LIS = lissencephaly, either severe (LIS_sev) or moderate (LIS_mod) with or without subcortical band heterotpia (SBH); LCH = lissencephaly with cerebellar hypoplasia; (iii) Central-PMG = central polymicrogyria-like cortical dysplasia and Central-Pachy = central pachygyria; (iv) Generalized PMG = generalized polymicrogyria and PMG_multi = multifocal polymicrogyria; and (v) Symp_Gyr = simplified gyral pattern with focal polymicrogyria.
Tubulin mutations groups were assigned according to structural modelization and biochemical data, in five subgroups, Group A: GTP binding pocket, nucleotide binding is essential for protein folding, heterodimer stability, and microtubule dynamics; Group B: longitudinal interactions; Group C: lateral protofilament interactions (residues involved in longitudinal and lateral interactions are necessary for both heterodimer and microtubule stability; Group D: microtubule-associated protein and motor protein interactions; and Group E: tubulin folding.

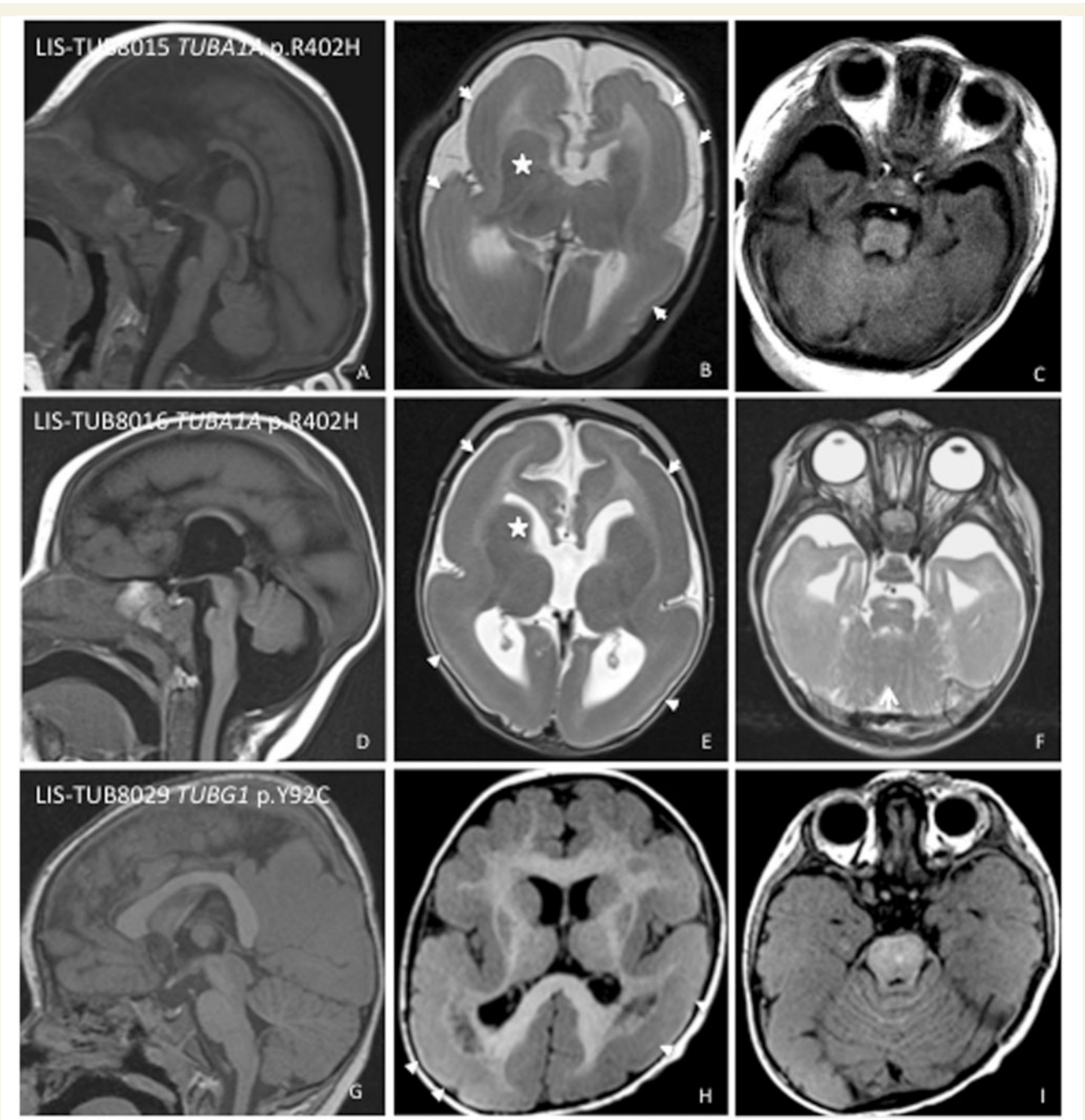

Figure 2 Lissencephaly. In this series of brain magnetic resonance illustrations, multiple images from the same patient are shown: Patient LIS-TUB_015 age 6 months (**A–C**), Patient LIS-TUB_016 age 4 months (**D–F**), and Patient LIS-TUB_029 age 4 years (**G–I**). For each patient, we selected midline sagittal images (**A**, **D** and **G**), axial images through the deep nuclei (**B**, **E** and **H**) and cerebellar vermis (**C**, **F** and **I**). This figure shows three cases with a lissencephaly pattern with the recurrent p.R402H *TUBA1A* mutation (**A–C**) and (**D–F**) and one with p.Y92C *TUBG1* mutation. All have agyria-pachygyria consistent with classic lissencephaly with a posterior more severe than anterior gradient (arrowheads). Other features include a dysmorphic corpus callosum (**A**, **D** and **G**) and non-visible internal capsules (white stars). Both patients with p.R402H *TUBA1A* mutations (**A** and **D**) also had moderate (**A**) to severe (**D–F**) vermian hypoplasia (arrow).

Two distinct patterns of malformation were observed; lissencephaly with or without moderate to severe cerebellar hypoplasia and dysplasia. The former condition is reminiscent of lissencephaly with cerebellar hypoplasia previously reported (Ross *et al.*, 2001).

Agyria-pachygyria: Fourteen patients (including eight foetuses) had severe lissencephaly corresponding to LIS grade 1–2 with thick cortex with a posterior to anterior gradient of severity and five had moderate lissencephaly corresponding to LIS grade 3–4 (including two with subcortical band heterotopia)

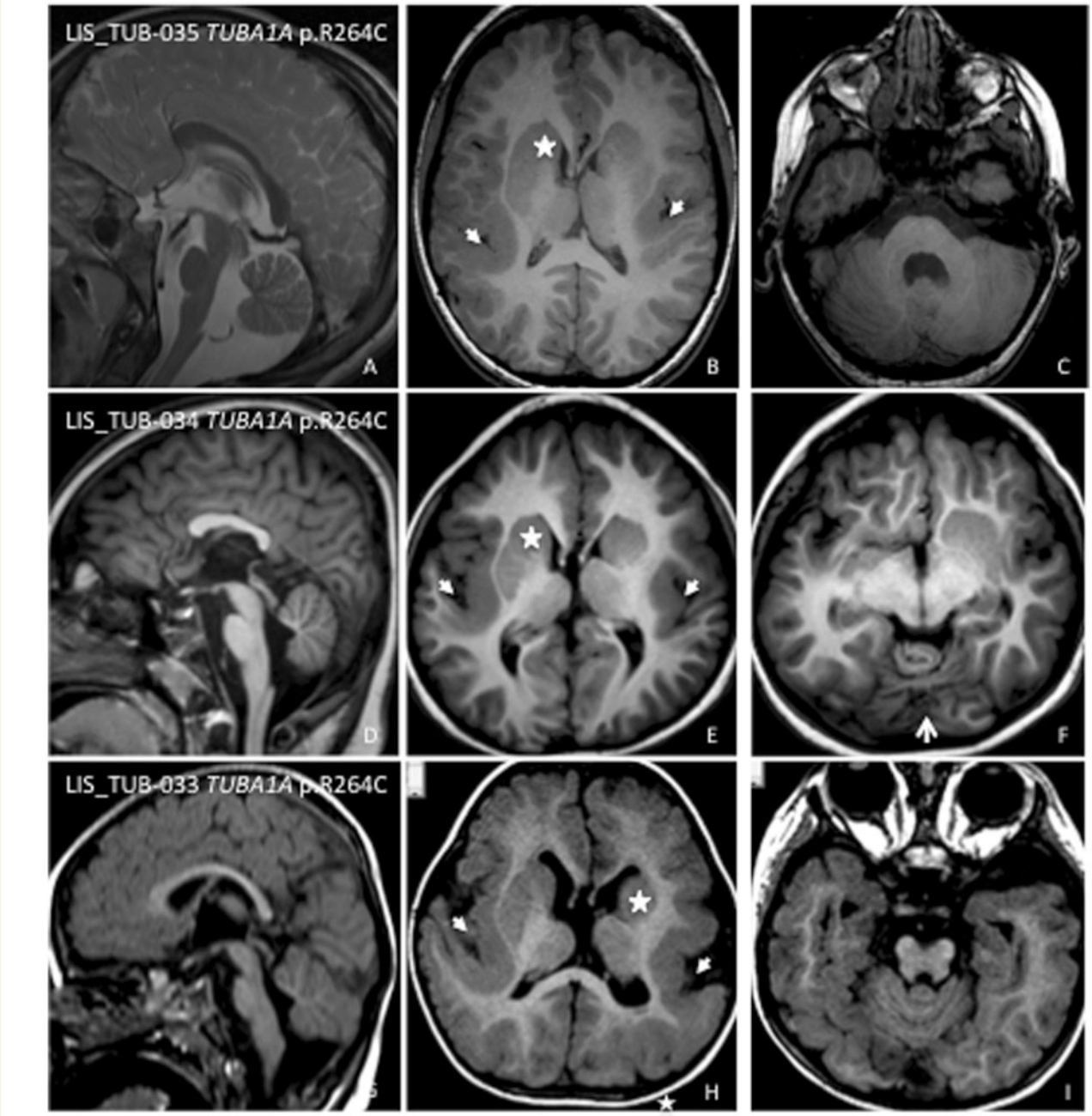

Figure 3 'Central' pachygyria with p.R264C *TUBA1A* mutations. This figure shows three patients with 'central' pachygyria and *TUBA1A* missense R264C mutations. Patient LIS_TUB-035 age 6 years (**A–C**), Patient LIS_TUB-034 age 6 years (**D–F**) and Patient LIS_TUB-033 age 13 months (**G–I**). For each patient, we selected midline sagittal images (**A**, **D** and **G**), axial images through the deep nuclei (**B**, **E** and **H**) and cerebellar vermis (**C**, **F** and **I**). All have pachygyria that appears mildly asymmetric and most severe over the central regions rather than over the posterior pole (white arrowheads). The basal ganglia are malformed and dysmorphic appearing as round structures in which the caudate, putamen and globus pallidus cannot be distinguished (white stars). Associated malformations include partial agenesis of the rostrum and the splenium (**D**), hypoplastic thin corpus callosum, thin brainstem with a flat pons (**G**), and mild (**A–D**) vermian hypoplasia with dysplasia (**F**) (arrow).

or moderate lissencephaly (with subcortical band heterotopia in Patient LIS_TUB_026). In this pattern, the basal ganglia appeared roughly normal in the majority of cases (14/19; 73.7%), although the anterior limb of the internal capsule was not visible. In this subtype, the malformation was always bilateral and showed a generally symmetrical distribution between hemispheres (Fig. 2). The lateral ventricles were often severely enlarged but were regularly shaped and symmetrical, in contrast with perisylvian pachygyria and polymicrogyria-like cortical dysplasia.

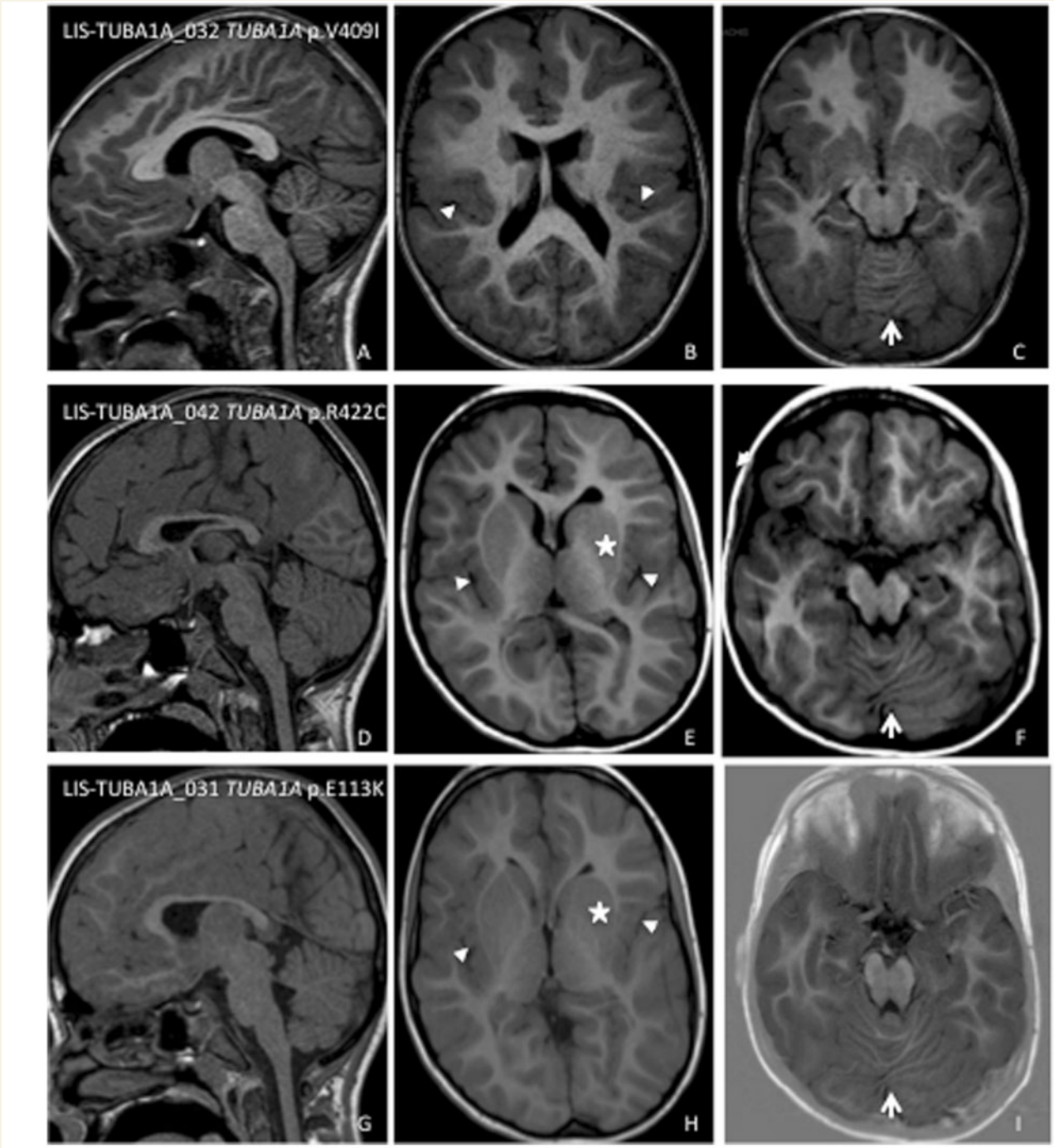

Figure 4 'Central' pachygyria. This figure shows three patients with 'central' pachygyria and *TUBA1A* missense mutations: Patient LIS-TUB_032 age 4.5 years (p.V409I, **A–C**), Patient LIS-TUB_042 age 3 years (p.R422C, **D–F**) and Patient LIS-TUB_031 age 10 years (p.E113K, **G–I**). All have pachygyria that appears mildly asymmetrical (**E**) and most severe over the central regions (white arrowheads). The basal ganglia are dysmorphic, appearing as round structures in which the caudate, putamen and globus pallidus cannot be distinguished (**E** and **H**) (white stars). Associated malformations include partial dysmorphism or thinning (**G**) of the corpus callosum, and vermian dysplasia (**C**, **F** and **I**) (white arrows).

Cerebellar and brainstem abnormalities: Malformations of the cerebellum were frequent in this subtype, ranging from severe vermian dysplasia (8/19; 42.1%) with preservation of the hemispheres, to milder vermian hypoplasia (6/19; 31.6%). Five had a normal cerebellum. The brainstem was frequently mildly to moderately hypoplastic (9/19; 47.4%) or severely hypoplastic with a flat pons (5/19; 26.3%) (Fig. 2).

Callosal abnormalities: Malformations of the corpus callosum mainly included a dysmorphic or hypoplastic corpus callosum (5/11; 45.5%) or hypogenesis or partial agenesis of the corpus

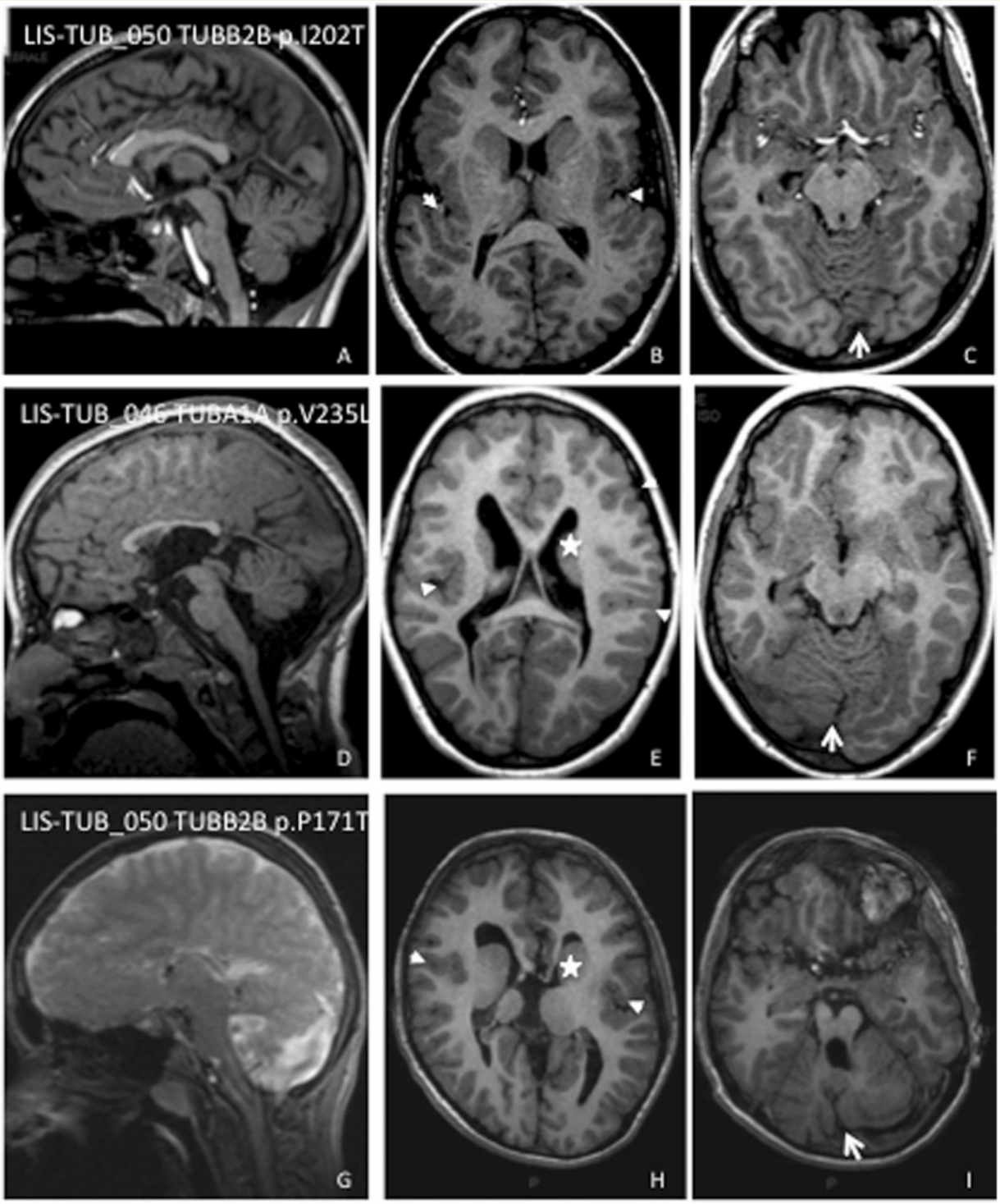

Figure 5 'Central' polymicrogyria-like cortical dysplasia. This figure shows three patients with central polymicrogyria-like cortical dysplasia, two with TUBB2B mutations: Patient LIS-TUB_050 age 15 years (**A–C**), Patient LIS-TUB_046 age 6 years (**D–F**) and one with *TUBA1A* mutation: Patient LIS-TUB_051 age 16 years (**G–I**). For each patient, we selected midline sagittal images (**A**, **D** and **G**), axial images through the deep nuclei (**B**, **E** and **H**) and cerebellar vermis (**C**, **F** and **I**). All have polymicrogyria that appear typical with an irregular surface of cortex or overfolded cortex aspect and irregularity at the grey-white interface (**B** and **E**) or atypical with a coarse aspect (**H**). The polymicrogyria appear mildly asymmetrical and most severe over the central (mid- and posterior frontal, perisylvian and anterior parietal) regions rather than over the posterior pole (white arrowheads). The frontal horns of both lateral ventricles are dysmorphic with malformed basal ganglia (mostly in **E** and **H**) (white stars). The corpus callosum is hypogenetic (**D**) or thin (**G**). The superior vermis is dysplastic in all cases (**C**, **F** and **I**) (white arrows).

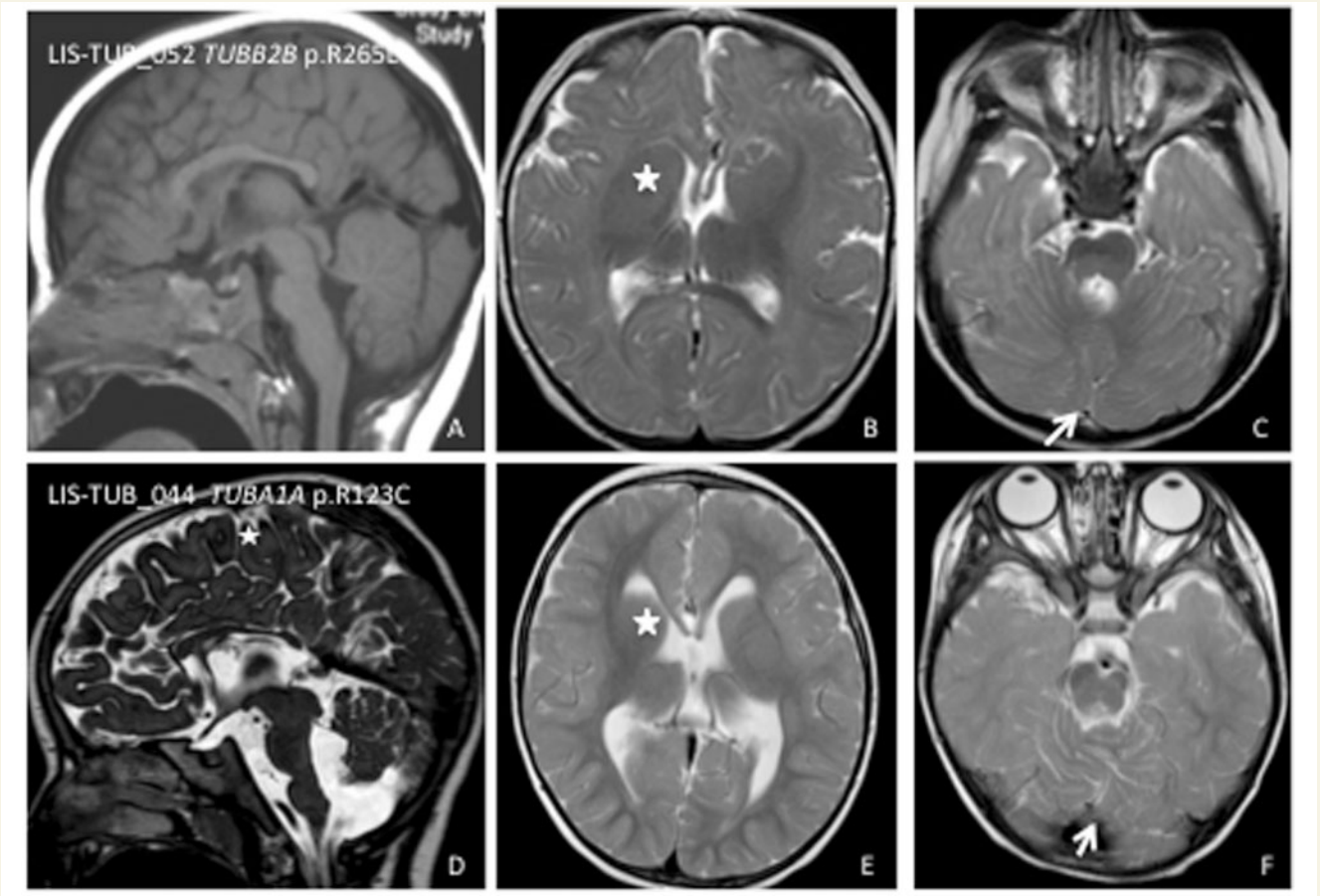

Figure 6 'Central' polymicrogyria-like cortical dysplasia in a poorly myelinated brain. This figure shows two patients with centrally predominant polymicrogyria-like cortical dysplasia with *TUBB2B and TUBA1A* mutations. Each row shows multiple images from the same patient; Patient LIS-TUB_052 (**A–C**), Patient LIS-TUB_044 (**D–F**) age 4 and 13 months, respectively. For each patient, we selected midline sagittal images (**A**, **D** and **G**), axial images through the deep nuclei (**B**, **E** and **H**) and cerebellar vermis (**C**, **F** and **I**). All cases show an abnormally thick sylvian and perisylvian cortex with a bumpy appearance at the surface and at the cortical-white matter junction. The frontal horns of both lateral ventricles are dysmorphic with hypertrophic and malformed basal ganglia (white stars). The corpus callosum is dysmorphic (**A**) or thin (**C**). The superior vermis is dysplastic in both cases (**C** and **F**) (white arrows).

callosum (6/11; 54.5%) in living patients, whereas all the eight foetal cases showed complete agenesis.

At last follow-up, the 11 living patients of this group were between 1 and 31 years of age (mean age: 9.95 years; median 7). In comparison to the patients with perisylvian pachygyria/polymicrogyria-like and simplified gyral subtypes, patients with the lissencephaly subtype tended to have more severe delay in both cognitive and motor development. All showed severe motor and speech delay, were either wheelchair-bound with no voluntary motor control (4/11; 36.4%) or had head control only (3/11; 27.3%), had no eye contact and no speech development, although three patients were able to walk unaided. All of the patients had severe epilepsy, which typically had an earlier onset and greater severity compared with the other subtypes. All had an early epileptic encephalopathy with infantile spasms, with onset from the neonatal period to 6 months of age (median 1 month). Several different seizure types were observed, with most patients having infantile spasms and tonic seizures except two who also experienced myoclonic seizures and absences. Seizures were refractory in all cases except one (Patient LIS_TUB_026 who showed the milder form of lissencephaly combined with subcortical band heterotopia, and presented early onset infantile spasms that were controlled with oral steroids and valproate). Most patients in this group had congenital microcephaly (9/11; 81.8%) with a head circumference ~3.2 standard deviations (SD) below the mean at birth. All had severe axial hypotonia, or mixed central hypotonia with limb spasticity. Of note, two also had facial diplegia and strabismus suggestive of pseudobulbar palsy.

At the genetic level, most patients (15/19, 78.9%) with this subtype carried mutations in *TUBA1A* mutations, whereas one foetus had a *TUBB2B* mutation (p.G58R). The other three cases had *TUBG1* mutations, with a phenotype almost indistinguishable from the others. Of note, however, these three patients had a normal brainstem and cerebellum. As previously reported (Bahi-Buisson *et al.*, 2008; Kumar *et al.*, 2010), the major

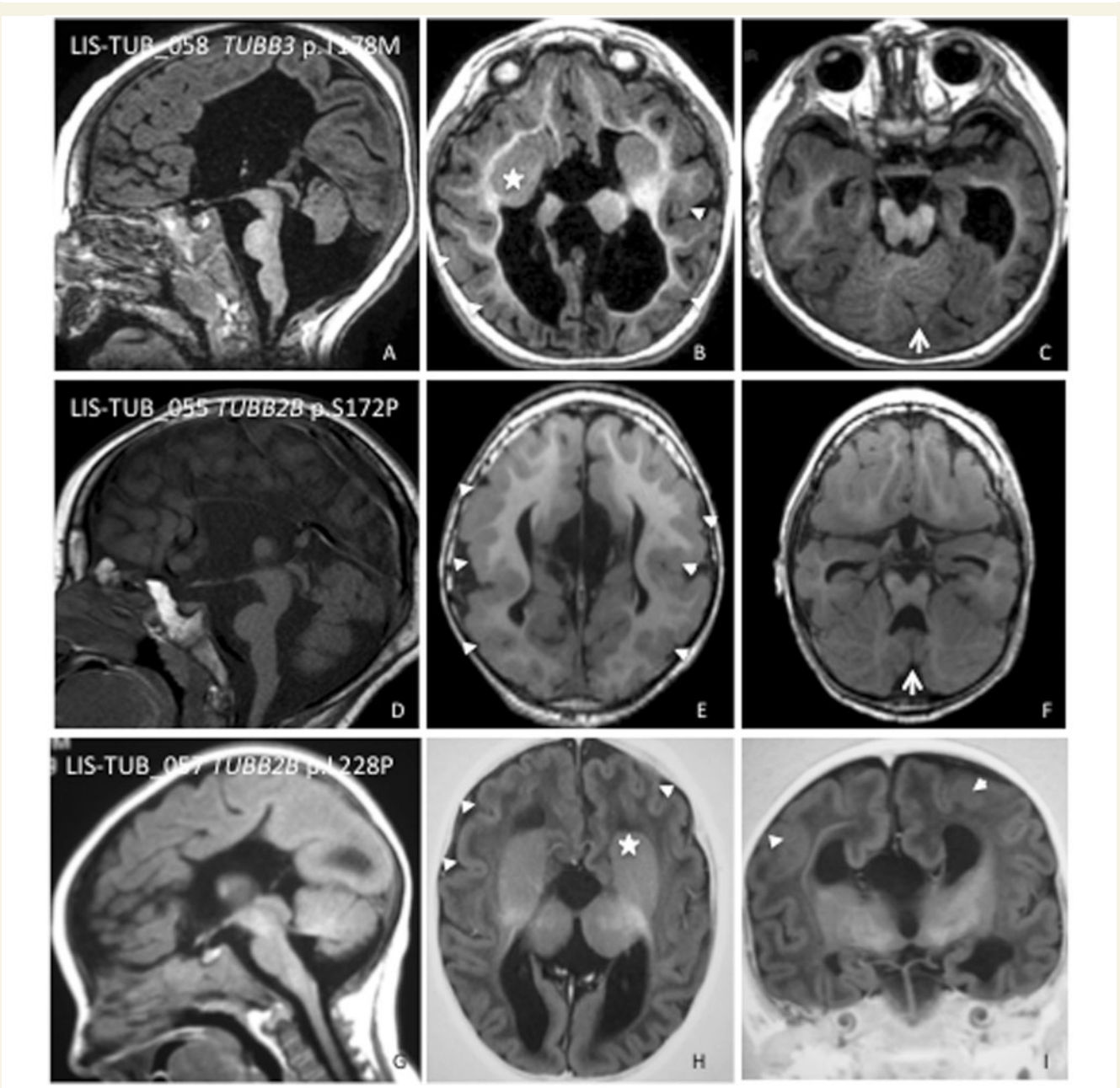

Figure 7 Generalized polymicrogyria-like cortical dysplasia. This figure shows three patients with generalized polymicrogyria-like cortical dysplasia with *TUBB3* mutations (**A–C**) and *TUBB2B* (**D–F** and **G–I**). Each row shows multiple images from the same patient: Patient LIS-TUB_058 (**A–C**), Patient LIS-TUB_055 (**D–F**) and Patient LIS-TUB_057 age 3 years, 3 years and 4 months, respectively. For each patient, we selected midline sagittal images (**A**, **D** and **G**), axial images through the deep nuclei (**B**, **E** and **H**) and cerebellar vermis (**C** and **F**); where images were not available, coronal images through the cerebellum are shown instead (**I**). In two cases (**B** and **E**) the cortex shows a coarse appearance, with excessively folded gyri (arrowheads). In the last case (**H**), (the youngest patient aged 4 months), the cortical surface is irregular with undersulcation and a variably thick polymicrogyria-like cortex (arrowheads). The polymicrogyria is extensive in 2/3 cases (**B** and **H**) with only few subnormal sulci or generalized without any areas of normal cortex (**E**) (white arrowheads) and associated with complete agenesis of corpus callosum, dysmorphic basal ganglia (white stars) and vermian cerebellar dysplasia (white arrows).

TUBA1A mutation responsible for this subtype affects the Arg402 residue leading to the recurrent mutation p.R402H (in 5/15) or p.R402C (in 2/15). Another recurrent mutation p.R422H was found in 2/15 patients.

Central pachygyria and polymicrogyria-like cortical dysplasia

This subtype corresponds to a pattern of malformation that is clearly distinguishable by the three following characteristic imaging

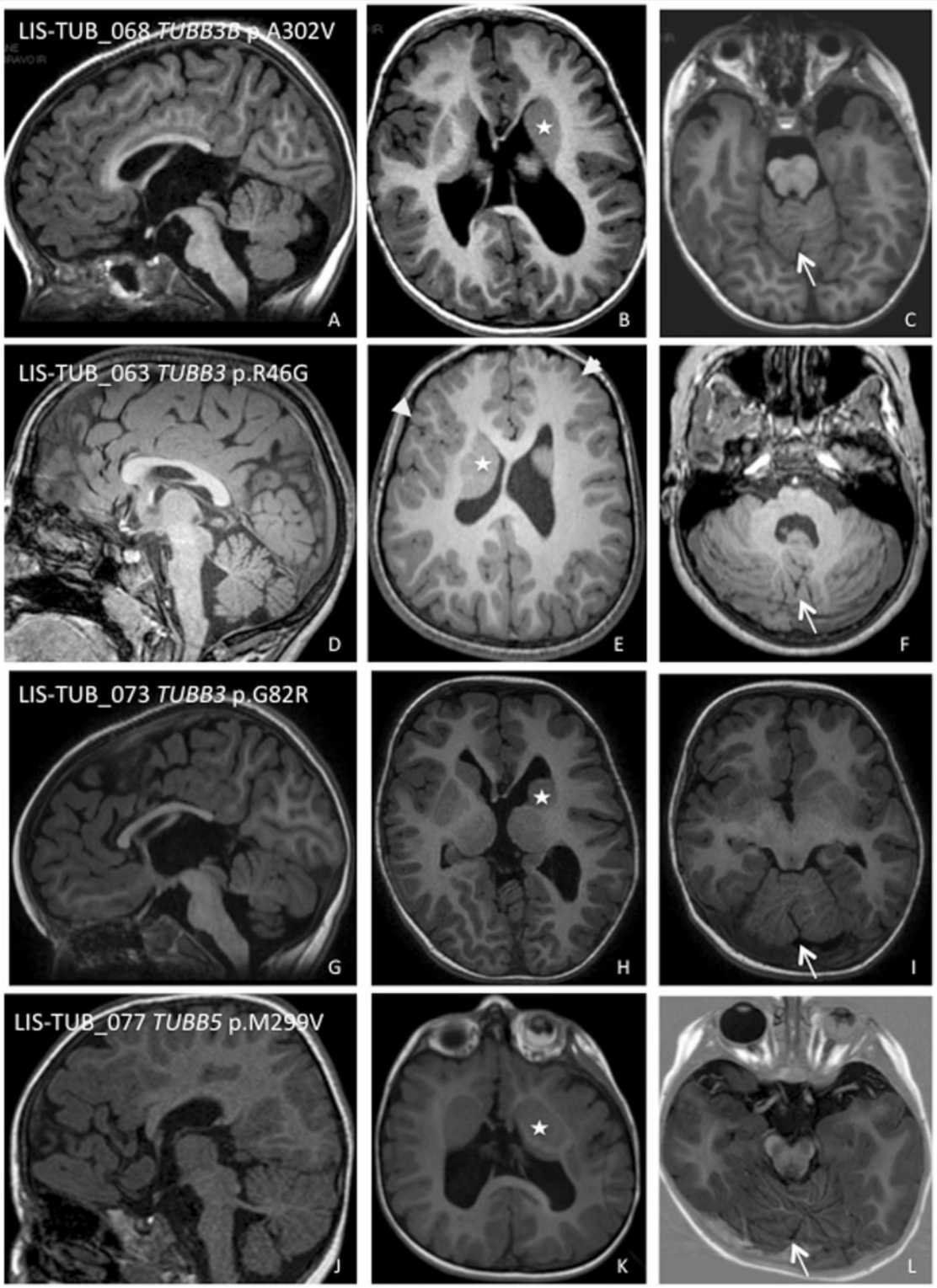

Figure 8 Gyral disorganization with multifocal dysplasia. This figure shows four patients with generalized polymicrogyria with *TUBB3* (Patient LIS-TUB_068 *TUBB3* age 3 years **A–C**, Patient LIS-TUB_063 *TUBB3* age 11 years **D–F** and Patient LIS-TUB_073 age 3 years **G–I**, respectively) or *TUBB5* mutations (Patient LIS-TUB_077 age 2 years, **J–L**). For each patient we selected midline sagittal (**A**, **D**, **G** and **J**) images, axial images through the deep nuclei (**B**, **E**, **H** and **K**) and cerebellar vermis (**C**, **F**, **I** and **L**). In all cases, the cortex displays an abnormal appearance with poorly folded gyri, generalized undersulcation (mostly the ternary sulci), with focal variably thick aspect reminiscent of focal dysplasia or atypical polymicrogyria (white arrows). In all cases also, the basal ganglia are malformed and the lateral ventricles are dysmorphic (white stars), and the vermis is dysplasic (white arrows). The corpus callosum is hypogenetic (**A–G**) or dysmorphic (**J**).

findings that define this group, comprising 22 living foetuses and two foetuses.

Bilateral 'central' cortical malformation more severe in posterior frontal, perisylvian and parietal regions and sparing the occipital cortex: In 13 cases (10 males, three females), this cortical malformation was reminiscent of pachygyria with a thick cortex and cortical infolding (Figs 3 and 4). In these cases, the cortex seemed thick whatever the age of MRI, excluding the misleading pattern of polymicrogyria due to immature myelination (Takanashi and Barkovich, 2003). In 11 other patients (including two foetuses), the malformation was more suggestive of polymicrogyria, although all the characteristics of this were not always present. These cases were defined as polymicrogyria-like cortical dysplasia (Fig. 5). Both pachygyria- and polymicrogyria-like cortical dysplasia were both bilateral in all patients, although asymmetrical in the majority. The lateral ventricles were often dysmorphic, especially anteriorly and were also asymmetrical in most patients.

Basal ganglia dysmorphy: All patients had malformed basal ganglia appearing as large round structures in which the caudate, putamen and globus pallidus could not be distinguished. Lack of clear separation between the caudate and putamen and bilateral hypoplasia of the anterior limbs of the internal capsule was also a major feature (Figs 3–5).

Cerebellar vermis and brainstem abnormalities: Vermian malformations were common while cerebellar hemispheres were always normal. This included mild vermian hypoplasia (9/24; 37.5%) or dysplasia (5/24; 20.8%), and less frequently severe vermian hypoplasia (3/24; 12.5%). The brainstem was commonly mildly hypoplastic with a flat pons (19/24; 79.2%) (Figs 3–5).

Callosal abnormalities: Malformations of the corpus callosum mainly consisted of a dysmorphic thin (7/24; 29.2%) or hypogenetic (5/24; 20.8%) corpus callosum, and less frequently partial (3/24; 12.5%) or complete (1/24; 4.2%) corpus callosum agenesis. Of note, the patient with corpus callosum agenesis was one of the two foetal cases whereas the others had a normal corpus callosum.

For the 22 living patients (of 24 cases) including 14 males and eight females, age at the time of last follow-up ranged from 1 to 17 years (mean 6.72 years; median 6.25 years). Moderate to severe motor delay was observed in all children. All patients had delayed sitting and standing in the first year, although all children older than 2 years were cruising or walking. Motor function in children older than 3 years ranged from assisted walking with a combination of a spastic and ataxic gait to independent toe walking. All children older than 3 years of age had severe speech delay, with a combination of dysarthric speech or expressive language impairment due to facial diplegia. Among the six children under 3 years, three developed babbling with meaningful communication. The majority (16/22; 72.7%) had significant microcephaly (between −3 to −5 SD below the mean). None had a normal neurological examination at the time of last follow-up. They had either isolated axial hypotonia (3/22; 13.6%) or combined with spastic diplegia (17/22; 72.3%) or tetraplegia (3/22; 13.6%). Five patients had epilepsy starting in the first year of life that became refractory in three cases. The three patients that experienced drug-resistant epilepsy had focal daily seizures with repeated status epilepticus, whereas the other two had generalized clonic seizures in one case, and focal motor seizure in the other. Seizure control was achieved with valproate in the first patient and carbamazepine in the second. Three had occasional seizures, and one of these had febrile seizures. In contrast with the agyria-pachygyria subtype, seizures were mainly focal or multifocal and no cases of infantile spasms or myoclonic seizures were reported. Only EEG tracing of patients with controlled epilepsy could be reviewed. In both cases, the EEGs were characterized by non-specific pattern consisting of slow and monotonous background activity (Supplementary Fig. 1).

As far as molecular data are concerned, strikingly, most patients with a pattern of central pachygyria (7/13; 53.8%) carried the same recurrent mutation p.R264C in *TUBA1A* (Fig. 3). The other mutations were not recurrent (p.E113K, p.R422C, p.A369T, p.D396Y, p.L397P, p.G436R, p.V409I). By contrast, half of the patients (5/11) with 'central' polymicrogyria-like cortical dysplasia carried mutations in *TUBB2B*. Patients with similar neuroimaging findings were found to have the same *TUBB2B* mutation (p.I202T). The other six patients had *TUBA1A* mutations (Table 1).

Generalized polymicrogyria-like cortical dysplasia

This subtype ($n = 6$, including three foetuses) was characterized by generalized polymicrogyria-like cortical dysplasia with complete or near-complete involvement of the entire cerebral cortex, without any region of maximal involvement or gradient of severity (Figs 6 and 7). Enlarged ventricles and dysmorphic basal ganglia with fusion between the caudate and putamen were observed in the majority of patients (5/6; 83.3%). In this subtype, most patients showed severe vermian and hemispheric dysplasia (4/6; 66.7%). The brainstem was severely hypoplastic with a flat pons in all cases. Also, in this subtype, all patients had complete agenesis of corpus callosum which is also a consistent feature in microlissencephaly.

At the last follow-up, the three children (one male and two females) were 1, 3 and 5 years of age, respectively. In comparison to other subtypes, patients with the generalized polymicrogyria-like cortical dysplasia resembled those with the agyria-pachygyria subtype. All patients had no motor or social development. Similarly, all had early onset epileptic seizures with infantile spasms, starting in the neonatal period. Seizures were refractory in all cases. All had congenital microcephaly with a head circumference between 4 and 5 SD below the mean at birth. All had axial hypotonia or mixed central hypotonia with limb spasticity, and two showed abnormal eye movements symptomatic of severe amblyopia.

The majority of patients with diffuse polymicrogyria-like cortical dysplasia were found to carry mutations in *TUBB2B* (4/6) whereas the remaining patients had *TUBA1A* and *TUBB3* mutations not found in other groups of cortical malformation syndromes (Table 1).

Simplified gyral pattern with area of focal polymicrogyria-like cortical dysplasia

This pattern that represents a milder form of tubulinopathy was found in 19 patients (12 males, seven females), including two inherited cases; one with father to son, and the other with mother to daughter transmission.

In this subtype, the most prominent feature was patchy multifocal atypical polymicrogyria over both hemispheres with a simplified gyral pattern or irregular sulcal pattern (Fig. 8). Although there was no clear specific pattern concerning gyral abnomalities distribution, the focal polymicrogyria-like cortical dysplasia was in all cases predominantly located in perisylvian and fronto-temporal regions. Also, in some cases (7/19; 36.8%) the distribution. was asymmetrical. Moderately enlarged and dysmorphic lateral ventricles were consistent features, as well as dysmorphic basal ganglia with fusion between the caudate and putamen. The corpus callosum was usually hypoplastic with a thin (6/19; 31.6%) or thick (1/19; 5.2%) appearance, whereas 11 had either hypogenesis (8/19; 42.1%) or partial corpus callosum posterior agenesis (3/19; 15.8%).

One patient (Patient LIS_TUB_059) also showed periventricular non-confluent nodular heterotopia. Of note, in this subtype, the cerebellar superior vermis was dysplastic in 15/19 cases (78.9%) and associated with hemispheric dysplasia in three cases. The brainstem was mildly hypoplastic in 5/19 cases (26.3%).

At the last follow-up, the 19 patients (12 males and seven females) in this subtype were 9 months to 40 years of age (median 5 years; mean 11.3 years). Motor delay was observed in all cases although the majority (17/19; 89.5%) were able to walk either with minimal support (10 cases) or unaided (seven cases). Among them, a spastic and ataxic gait was noted in seven (36.8%). All had moderate to severe intellectual disability and attended a special school. Interestingly, the three children with familial disorders presented with minimal intrafamilial variability although at referral, they displayed severe hypotonia and an ataxic gait. Head circumference was within the normal range in the majority (13/19; 68.4%), whereas six patients had significant and severe microcephaly from birth (less than −2.5 SD below the mean). Twelve had subtle neurological signs with mild truncal hypotonia, whereas the remaining had spastic diplegia or tetraplegia and orofacial dyspraxia. Intermittent or permanent strabismus was a frequent finding (15/19; 78.9%). In contrast with the other subtypes, only three patients developed a severe epileptic encephalopathy, and among them only one is refractory. Only five (5/19; 26.3%) had occasional seizures including one case of febrile seizures. EEG tracing could be reviewed in four patients with controlled seizures. In all cases, we identified non-specific EEG patterns consisting of slow and monotonous background activity, unusual asynchrony of sleep pattern or posterior slow theta rhythm with intermixed spikes (Supplementary Figs 2–4).

About half of the patients (9/19; 47.4%) with 'simplified' gyral and multifocal polymicrogyria-like cortical dysplasia had *TUBB3* mutations. The remaining cases carried *de novo* mutations either in *TUBB2B* (6/19; 31.6%) or *TUBB5* (3/19; 15.8%). Remarkably, one patient also had a *TUBA1A* mutation (p.V353I) (Table 1). Of note, all patients with *TUBB5* mutations had microcephaly (2/3) compared to others (3/6 in *TUBB2B* and 1/9 in *TUBB3*, respectively). Similarly, only patients with *TUBB2B* mutations had severe cerebellar dysplasia that was not observed in other patients with *TUBB3* and *TUBB5* mutations.

Discussion

This study describes the largest cohort of patients yet reported with malformations of cortical development related to *TUBA1A*, *TUBB2B*, *TUBB3*, *TUBB5* and *TUBG1* genes, collectively known as tubulinopathies. Six years after the discovery of *TUBA1A*, the phenotypes associated with each gene have significantly evolved from clear splitting of each tubulin-associated malformation to a recent lumping concept of overlapping tubulinopathies. In this study, we examined the clinical and brain MRI characteristics of 80 individuals harbouring 61 distinct mainly *de novo* mutations in the different tubulin genes, associated with cortical malformations, and highlight the following findings.

Firstly, this study together with data from literature indicates the presence of similarities and specific features defining the key features of the 'tubulinopathy spectrum'. These include dysmorphic basal ganglia, hypoplasia or agenesis of the corpus callosum, brainstem and cerebellar hypoplasia. Also, the emerging concept of polymicrogyria-like cortical dysplasia that is unique in tubulin-related cortical dysgenesis is worth considering when assessing brain magnetic resonance images of patients with diffuse cortical malformations. Secondly, although the range of brain developmental defects is wider than originally described, mutations in each tubulin gene are responsible for some predominant phenotypes. They include a significant proportion of foetal cases with microlissencephaly and at the other end of the spectrum, patients with mild intellectual disability, focal polymicrogyria and abnormal gyral patterning and peripheral neuropathies. Thirdly, there is clear evidence for phenotype–genotype correlation and this gives us some insight into the mechanisms underlying tubulinopathies.

Key features of tubulinopathies

Dysmorphism or unusual orientation of the basal ganglia (60/80; 75%) is one of the pathognomonic features of tubulinopathies. It is suspected to result from abnormal axon guidance of the corticospinal tract through the internal capsule (Bahi-Buisson *et al.*, 2008; Barkovich, 2013; Cushion *et al.*, 2013). This appearance is the result of a combination of a dysgenesis of the anterior limb of internal capsule with a head of the caudate protruding into the ventral horn of the ventricles. Consequently, the lateral ventricles are enlarged with a hooked aspect of the anterior horn. This is an easily recognizable feature on brain MRI and increasing awareness should steer clinicians and neuroradiologists in the direction of specific molecular genetic testing. Of note, the thalamus is usually less enlarged and this sign is particularly visible in association with cortical malformations of mild to moderate severity, and more subtle in lissencephalies.

Corpus callosum anomalies either partial to complete agenesis or hypoplasia (32/80; 40%) are also dominant features in tubulinopathies. We and others proposed that they are the result of the combination of abnormal corticogenesis, either impaired migration or lamination, as well as abnormal growth cone dynamics of callosal axons (Jaglin and Chelly, 2009; Barkovich, 2013). This is further reinforced by the fact that the severity of corpus callosum abnormalities seems to be related to the severity of cortical dysgenesis, either lissencephaly, microlissencephaly or generalized

polymicrogyria-like cortical dysplasia (25/37; 67.6% in our series and 39/63; 61.9% including literature data). Conversely, only a few cases with multifocal polymicrogyria or pericentral pachygyria or polymicrogyria-like cortical dysplasia demonstrate complete (1/33; 3% in our series and 3/46; 6.5% including literature data) or partial corpus callosum agenesis (3/33; 9% in our series; 3/46;6.5% including the literature data) (Morris-Rosendahl *et al.*, 2008; Kumar *et al.*, 2010; Jansen *et al.*, 2011; Cederquist *et al.*, 2012; Guerrini *et al.*, 2012; Mokanszki *et al.*, 2012; Sohal *et al.*, 2012; Amrom *et al.*, 2013; Cushion *et al.*, 2013; Okumura *et al.*, 2013; Hikita *et al.*, 2014). Remarkably, other projection neurons, particularly corticofugal projection neurons are also particularly affected in tubulinopathies as shown by the severe brainstem hypoplasia in tubulinopathies. These neurons project away from the cortex but do not cross the midline, and project both subcortically to deeper brain areas, and subcerebrally to brainstem and spinal cord targets.

Polymicrogyria in tubulinopathies

From the seminal description of 'polymicrogyria' in tubulinopathies (Jaglin and Chelly, 2009; Jaglin *et al.*, 2009), the imaging features of this cortical malformation show specific and original features that distinguish it from others. On MRI, the consensus criteria for the diagnosis 'typical' polymicrogyria combines the presence of regions of apparent cortical thickening with an irregular cortical surface and a 'stippled' grey–white junction, usually without associated T_2 signal change in patients who are fully myelinated (Barkovich *et al.*, 1999; Takanashi and Barkovich, 2003; Leventer *et al.*, 2010). However, a range of imaging appearances of polymicrogyria (gyral–sulcal dysmorphisms) is seen and can be divided into three main categories; coarse, delicate, and sawtooth polymicrogyria depending on morphologic appearance (Barkovich, 2010). Based on these classifications, *TUBA1A*, *TUBB2B*, *TUBB3* or *TUBB5*-related polymicrogyria more closely resemble coarse polymicrogyria with a thick cortex and irregular surfaces on both the pial and grey–white junction sides than other patients with polymicrogyria (Jaglin and Chelly, 2009; Jaglin *et al.*, 2009; Poirier *et al.*, 2010, 2013*b*; Breuss *et al.*, 2012; Amrom *et al.*, 2013; Cushion *et al.*, 2013). Of note, one of the distinctive signs of atypical polymicrogyria is the absence of deep infolding that is usually highly suggestive of polymicrogyria (Barkovich, 2010). These observations led Cushion *et al.* (2013) to propose the concept of atypical polymicrogyria or polymicrogyria-like cortical dysplasia. This is further reinforced by neuropathological anomalies of a foetal case of *TUBB2B*-related polymicrogyria that we have previously described (Jaglin and Chelly, 2009; Jaglin *et al.*, 2009; Cushion *et al.*, 2013). Histological features comprised disorganization of cortical layering, which is consistent with unlayered polymicrogyria, but also additional signs combining neuronal overmigration through breaches in the pial basement membrane and neuronal heterotopias more reminiscent of cobblestone lissencephaly rather than classic polymicrogyria (Jaglin and Chelly, 2009; Cushion *et al.*, 2013).

Importantly, we and others have found a significant number of patients with a milder neurological phenotype and only highly localized areas of irregular cortex, described as 'focal polymicrogyria'. In these patients, the main features reminiscent of a tubulinopathy, are the abnormal basal ganglia, corpus callosum abnormalities and cerebellar hypoplasia (Cushion *et al.*, 2013). These observations suggest that tubulinopathies may be responsible for a subset of children with corpus callosum abnormalities, either hypogenesis or dysmorphic and cerebellar hypoplasia without obvious cortical malformations. This group of malformations, particularly seen in *TUBB3* mutations, but also reported with *TUBB2B* and *TUBA1A* mutations (Kumar *et al.*, 2010; Cushion *et al.*, 2013), is complex and closer to phenotypes observed in mutations involved in congenital fibrosis of extraocular muscle disorders (Tischfield *et al.*, 2010, 2011; Chew *et al.*, 2013). Further studies in these latter groups are clearly needed. This group of malformations, is particularly seen in *TUBB3* mutations, but is also reported with *TUBB2B* and *TUBA1A* mutations (Kumar *et al.*, 2010; Cushion *et al.*, 2013).

The predominant phenotypes associated with mutations in each specific tubulin gene

Our data combined with the literature also emphasize that prominent and prevalent malformations of cortical development are associated with each mutated gene (Table 1).

The core phenotype of *TUBA1A*-related tubulinopathies (45 described here and 30 reported) consists of lissencephaly, most frequently classic (28/75; 37.3%) or with cerebellar hypoplasia (11/75; 14.7%) (Poirier *et al.*, 2007; Bahi-Buisson *et al.*, 2008; Fallet-Bianco *et al.*, 2008; Morris-Rosendahl *et al.*, 2008; Kumar *et al.*, 2010; Okumura *et al.*, 2012; Sohal *et al.*, 2012; Hikita *et al.*, 2013). Our data also show that a significant proportion of *TUBA1A* mutations cause microlissencephaly (10/75; 13.3%). More interestingly, they represent the first dominant aetiology of microlissencephaly, as other known genetic disorders, either *NDE1* or *WDR62* mutations, are of autosomal recessive inheritance (Bilguvar *et al.*, 2010). At the less severe end of the spectrum, 'central pachygyria' represents about one-third of our cohort (13/45; 28.9%), whereas this was not reported in other series (Bahi-Buisson *et al.*, 2008). Finally, in addition to the above highlighted phenotypes, the spectrum of *TUBA1A*-related cortical dysgenesis includes a low proportion of patients with either central (8/75; 10.7%) and less frequently generalized (2/75; 2.7%) polymicrogyria-like cortical dysplasia, or simplified gyral pattern with focal atypical polymicrogyria (3/75; 4%) (Jansen *et al.*, 2011; Cushion *et al.*, 2013; Poirier *et al.*, 2013).

One of the most striking cortical malformations associated with *TUBB2B* mutations (18 described here and 14 reported elsewhere) is polymicrogyria-like cortical dysplasia (28/32; 87.5%), either centrally predominant (12/28; 42.8%) or generalized (7/28; 25%). Alternatively, a significant proportion of *TUBB2B*-mutated patients demonstrate a milder cortical malformation consisting of focal polymicrogyria-like cortical dysplasia and simplified gyral pattern (9/28; 32.1%) that is also seen in *TUBB3* and *TUBB5* mutations. At the other end of the spectrum, *TUBB2B* tubulinopathies may be associated with microlissencephaly (3/32; 9.4%) or lissencephaly with agenesis of the corpus callosum (1/

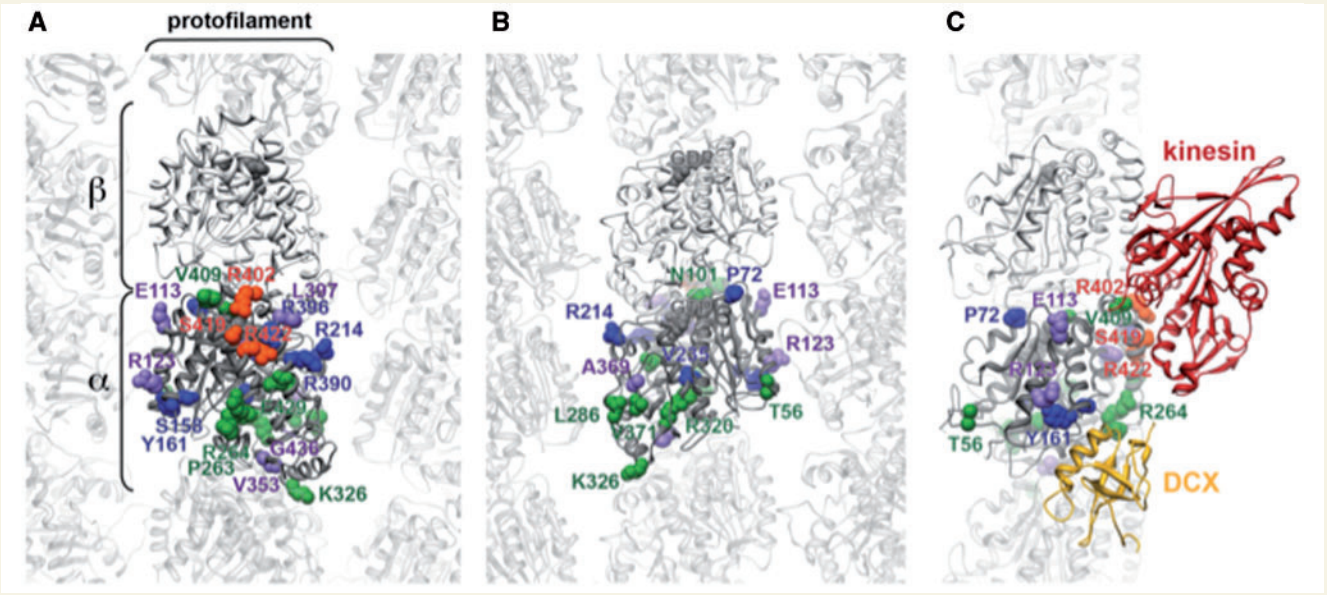

Figure 9 Localization of TUBA1A-mutated residues in the microtubule structure. (**A**) Microtubule structure visualized from the side, plus-end pointing up. The crystal structure of a tubulin dimer (grey ribbons, 1JFF.PDB) was fitted into a subnanometer resolution cryo-EM microtubule reconstruction (EMDB entry 1788), thus generating a pseudo-atomic model of the microtubule. Side-chains of TUBA1A mutated residues reported here are displayed as spheres, and coloured according to the phenotype associated with their mutations: agyria-pachygyria phenotype in red, lissencephaly with cerebellar hypoplasia in green, central pachygyria in purple, polymicrogyria phenotype in blue, simplified gyral pattern in black. GTP and GDP are displayed as grey spheres. The location of mutated residues and the nature of the substitution were used to predict the potential effect of mutations on microtubule assembly and interactions. (**B**) Microtubule structure visualized from the luminal side, plus end pointing up (180° rotation compared with **A**). Representation parameters as in **A**. (**C**) Single protofilament rotated 90° compared with **A**, and with plus-end pointing up. Representation parameters as in **A**. In addition, atomic structures of a kinesin motor domain (red ribbons, 1BG2.PDB) and DCX N-terminal DC domain (yellow ribbons, 1MJD.PDB) were displayed. Mutated residues associated with agyria-pachygyria (red), as well as V409 localize at the interface with kinesin, whereas R264 is in close proximity of DCX.

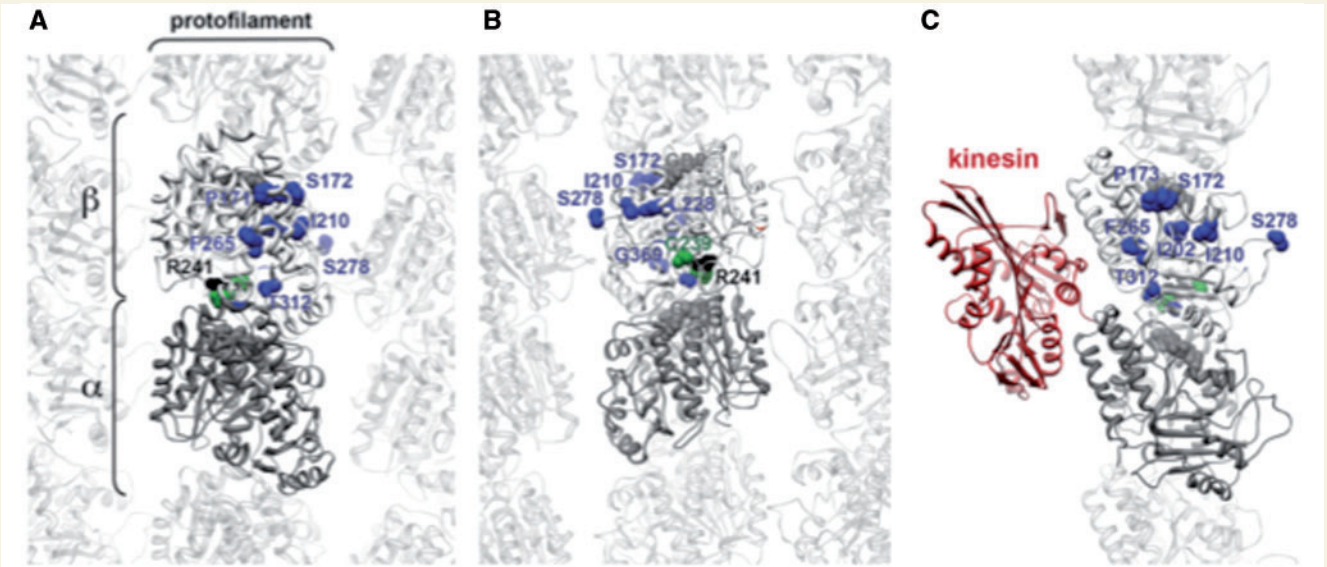

Figure 10 Localization of TUBB2B-mutated residues in the microtubule structure. (**A**) Localization of TUBB2B mutated residues in the microtubule structure visualised from the side, plus-end pointing up. Representation parameters are as in Fig. 9A. (**B**) Luminal view. (**C**) Single protofilament rotated 90° compared to **B**, and with plus-end pointing up. TUBB2B mutations reported here do not affect the microtubule-kinesin interface. Representation parameters as in Fig. 9C.

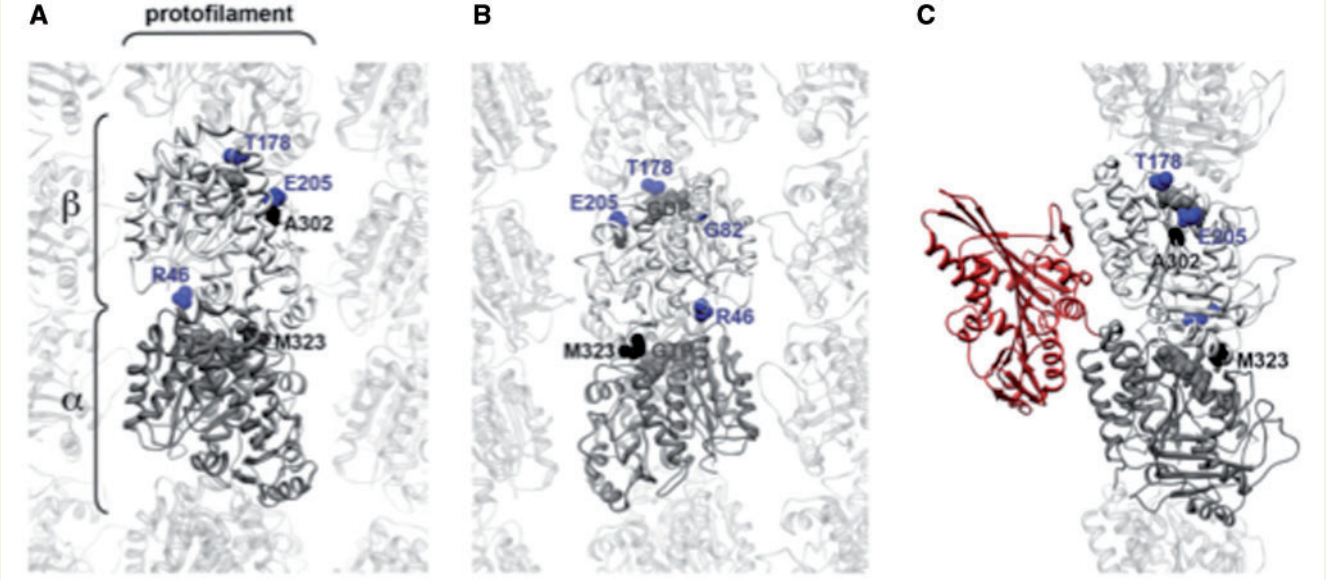

Figure 11 Localization of TUBB3 mutated residues in the microtubule structure. (**A**) Localization of TUBB3 mutated residues in the microtubule structure visualized from the side, plus-end pointing up. Representation parameters are as in Fig. 10A. (**B**) Luminal view. (**C**) Single protofilament rotated 90° compared to **B**, and with plus-end pointing up. TUBB3 mutations reported here do not affect the microtubule-kinesin interface. Representation parameters as in Fig. 9C.

32; 3.1%) (Cederquist *et al.*, 2012; Guerrini *et al.*, 2012; Romaniello *et al.*, 2012; Amrom *et al.*, 2013; Cushion *et al.*, 2013).

The spectrum of *TUBB3*-related tubulinopathies is wider than others as it encompasses ophthalmological and peripheral nerve pathologies that are not necessarily associated with cortical malformations (Poirier *et al.*, 2010; Tischfield *et al.*, 2010, 2011; Chew *et al.*, 2013). If we focus our attention on only cortical dysgenesis ($n = 11$), one of the most recognizable features is their milder severity with a majority of patients demonstrating focal or multifocal polymicrogyria-like cortical dysplasia with an abnormal and simplified gyral pattern (9/11; 81.8%). However, it is noteworthy that the remaining two patients with *TUBB3* mutations demonstrated extremely severe cortical dysgeneses, one foetal case showing microlissencephaly and the other, generalized polymicrogyria.

For *TUBB5* and *TUBG1* mutations, the number of patients with mutations in these genes is limited and conclusions are still difficult to draw. However, on the basis of available data, *TUBB5* tubulinopathies are also highly reminiscent of *TUBB3* cortical dysgenesis, with one of the most distinctive features of *TUBB5* being microcephaly associated with relative mild cortical dysgenesis (Breuss *et al.*, 2012). On the other hand, *TUBG1*-related cortical dysgenesis consists mainly of a pattern of classic lissencephaly with severe microcephaly that resembles *TUBA1A*-related lissencephaly (particularly those caused by p.R402C/H substitutions) (Poirier *et al.*, 2013*a*). One milder case demonstrated posteriorly predominant subcortical band heterotopia, a pattern previously observed in one case of *TUBA1A* mutation but with corpus callosum agenesis (Bahi-Buisson *et al.*, 2008; Poirier *et al.*, 2013).

Evidence for phenotype–genotype correlations in tubulinopathies

Our data, in combination with the literature (Tischfield *et al.*, 2011) emphasize that prominent and prevalent malformations of cortical development are associated with each of the mutated genes. These predominant tubulins' related phenotypes, as well as less frequent ones, are summarized in Table 1.

As far as genotype–phenotype correlations are concerned, our data also show that one of the consistent findings in both this study and data in the literature is that recurrent mutations result in similar phenotypes. Amongst *TUBA1A* mutations, two major recurrent mutations were found. The substitution p.R264C (7/45; 15.6% of *TUBA1A* mutations) is invariably associated with central pachygyria, and more interestingly is responsible for half of this malformation subtype. The second hot-spot of mutations, p.R402H (5/45; 11.1%) is invariably responsible for classic lissencephalies in our series and in the literature (Kumar *et al.*, 2010; Mokanszki *et al.*, 2012). Similarly, recurrent *TUBB2B* (p.S172P, p.I202T, p.F265L, p.A248V) and *TUBB3* mutations (p.R262H, p.E205K, p.E410K) also result in similar phenotypes, although their occurrence is less common (Tischfield *et al.*, 2010; Amrom *et al.*, 2013; Chew *et al.*, 2013).

Interestingly, mutation-related correlations are reinforced by the observation of distinguishable phenotypes resulting from different substitutions altering the same residue. For example, the most common *TUBA1A* substitution p.R264C, predominantly results in 'central pachygyria', whereas p.R264H causes microlissencephaly with complete agenesis of the corpus callosum, one of the most severe forms of tubulinopathy. Similarly, consequences of

Table 2 Clinical features of tubulinopathies subtypes

Phenotypes	45 *TUBA1A* 27 living 18 foetuses	18 *TUBB2B* 12 living 6 foetuses	11 *TUBB3* 10 living 1 foetus	3 *TUBB5* 3 living	3 *TUBG1* 3 living
Male	29	13	6	2	1
Female	16	5	5	1	2
Age min–max (years)	1–18	0.9–36	2–36	3–4.8	1.5–31
Motor impairment					
Total	26 (1 N/A)	12	10	3	3
Mild (mild spasticity/ataxia with minor impairment)	9 (34.6%)	4 (30%)	4 (40%)	0	0
Moderate (ability to walk independently or with minimal aid)	9 (34.6%)	4 (30%)	4 (40%)	3 (100%)	1 (33.3%)
Severe	8 (30.8%)	4 (30%)	2 (20%)	0	2 (66.7%)
Abnormal tone					
Total	27	12	10	3	3
Spastic diplegia or tetraplegia	23 (85.2%)	6 (50%)	3 (30%)	0	3 (100%)
Hypotonia	4 (14.8%)	3 (25%)	3 (30%)	3 (100%)	0
Epilepsy					
Total	27	12	10	3	3
Occasional seizures (or controlled epilepsy)	7 (25.9%)	4 (33.3%)	1 (10%)	1 (33%)	0
Refractory	10/27 (37%)	2 (16.7%)	2 (20%)	0	3 (100%)
Abnormal head size					
Total	25	12	10	3	3
Microcephaly (HC < -2SD)	22/25 (88%)	6 (50%)	2 (20%)	3 (100%)	2 (66.6%)
Major characteristics of brain malformations (MRI)					
Total	45	18	11	3	3
Classic lissencephaly[a]	15 (33.3%)	1 (5.6%)	0	0	3 (100%)
Microlissencephaly[b]	9 (20%)	2 (11.1%)	1 (9%)	0	0
Perisylvian pachygyria or polymicrogyria-like cortical dysplasia	19 (42.2%)	5 (27.8%)	0	0	0
Generalized polymicrogyria-like cortical dysplasia	1 (2.2%)	4 (22.2%)	1 (9%)	0	0
Multifocal polymicrogyria with or without simplified gyral pattern	1 (2.2%)	6 (33.3%)	9 (81.8%)	3 (100%)	0
Moderate to severe cerebellar vermis/hemisphere dysplasia and/or hypoplasia	18/45 (40%)	11/18 (61.1%)	11/11 (100%)	1/3 (33%)	0
Agenesis of corpus callosum (partial or complete)	20/45 (44.4%)	8/18 (44.4%)	3/11 (27.3%)	1/3 (33%)	0

[a]Lissencephaly includes classic lissencephaly with all degrees of severity, mild, moderate and severe and lissencephaly with cerebellar hypoplasia.
[b]Lissencephaly with cerebellar hypoplasia includes all degrees of severity, mild, moderate and severe.

recurrent substitutions p.R422H and p.R422C are distinguishable, because the former is responsible for lissencephaly whereas p.R422C causes central pachygyria (Kumar *et al.*, 2010). Similarly also, the *TUBB3* substitution p.R262C mostly results in an isolated restriction of eye movements, whereas p.R262H causes a severe ophthalmological disorder combined with a brain malformation. *In vitro* folding assays and overexpression in mammalian cells has demonstrated that the p.R262H mutation results in the generation of more tubulin heterodimers with higher levels of microtubule incorporation than p.R262C (Tischfield *et al.*, 2010, 2011). Perhaps in a similar manner, the mutation p.R264H that causes lethal microlissencephaly, one of the most severe brain malformations, compared to p.R264C, may also permit higher levels of heterodimer formation and microtubule incorporation. Thus, the consequences of the substituted residue may result in different changes in the function of tubulin, from drastic to milder modifications resulting in various cortical malformations.

To gain further insight into the genotype–phenotype relationships, we also performed additional analysis of the relationship between the predicted effects of mutations on *TUBA1A*, *TUBB2B* or *TUBB3* structure and function, taking into account local or global destabilization in the structure. Depending on their localization in the tertiary structure of tubulin, point mutations can be predicted to affect five distinct biochemical properties: nucleotide exchange and hydrolysis (GTP binding pocket), longitudinal and lateral protofilament interactions and microtubule–protein interactions with kinesin, dynein

Table 3 Tubulin mutations groups were assigned according to structural data and biochemical data

	Total	Group 1 severe This series ($n = 34$) + literature ($n = 64$) (+ *3 *TUBG1*)	Group 2 moderate This series ($n = 25$) + literature ($n = 30$)	Group 3 mild This series ($n = 15$) + literature ($n = 36$) (+ *3 *TUBB5*)
Gene (number of cases reported)	*TUBA1A* (75) *TUBB2B* (29) *TUBB3* (27) *TUBG1* (3) *TUBB5* (3)	*TUBA1A* (51) *TUBB2B* (11) *TUBB3* (2) *TUBG1* (3)	*TUBA1A* (21) *TUBB2B* (9)	*TUBA1A* (3) *TUBB2B* (9) *TUBB3* (25) *TUBB5* (3)
A: GTP binding	7/129 (5.4%)	7 (10.9%)	1 (3.3%)	0
B: Longitudinal interactions	12/129 (9.3%)	5 (7.8%)	3 (30%)	4 (12.5%)
C: Lateral protofilament interactions	15/129 (11.6%)	7 (10.9%)	5 (16.7%)	3 (8.3%)
D: MAP and motor protein interactions	65/129 (50.4%)	30 (46.8%)	17 (56.7%)	18 (50%)
E: Tubulin folding	31/129 (24%)	15 (23.4%)	4 (13.3%)	12 (33.3%)

Three groups of severity:
Group 1 (severe tubulinopathies) included classic lissencephaly and with cerebellar hypoplasia, microlissencephaly, and diffuse polymicrogyria-like subtypes; Group 2 (moderate tubulinopathies) comprises central polymicrogyria and pachygyria; and Group 3 (milder tubulinopathies), simplified gyral pattern and multifocal polymicrogyria. Patients previously reported in the literature (Morris-Rosendahl *et al.*, 2008; Kumar *et al.*, 2010; Tischfield *et al.*, 2010; Jansen *et al.*, 2011; Cederquist *et al.*, 2012; Guerrini *et al.*, 2012; Mokanszki *et al.*, 2012; Romaniello *et al.*, 2012; Sohal *et al.*, 2012; Amrom *et al.*, 2013; Chew *et al.*, 2013; Cushion *et al.*, 2013; Okumura *et al.*, 2013; Hikita *et al.*, 2014); MAP = microtubule associated protein.

and other microtubule-associated proteins and heterodimer stability (Lowe *et al.*, 2001; Tischfield *et al.*, 2011) (Figs 9–11 and Table 1). Overall, the large majority of *TUBA1A*, *TUBB2B* and *TUBB3* mutations are predicted to impair interactions with microtubule-associated proteins and motor proteins (28/75; 37.3%) here, and (64/129; 49.6%) including literature data) or tubulin folding (24/75; 32%) here and (31/129; 24%) including literature data.

We also examined whether a specific group of mutations could be related to the severity of cortical malformations. To investigate this question, we identified three groups, Group 1 (severe tubulinopathies) included classic lissencephaly with cerebellar hypoplasia, microlissencephaly and diffuse polymicrogyria-like subtypes ($n = 34$ in our series, 64 including reported cases), Group 2 (moderate tubulinopathies) comprised central polymicrogyria and pachygyria ($n = 25$ in our series, 30 including reported cases) and Group 3 (milder tubulinopathies) consisted of simplified gyral pattern and multifocal polymicrogyria subtypes ($n = 15$ in our series, 36 including reported cases). No significant differences were observed between the different subgroups. However, it is noteworthy that severe tubulinopathies were more often associated with tubulin mutations affecting the GTP binding pocket [7 (10.9%)], although these mutations were never found in milder phenotypes. By contrast, about a third of tubulin mutations leading to milder forms were predicted to impair tubulin folding [12/36 (33.3%), compared to a lower proportion in severe and moderate malformations (15; 23.4%) and (4; 13.3%), respectively (Table 1)].

Because tubulinopathies comprise a defect in axonogenesis and axon tract development as demonstrated by the high frequency of corpus callosum dysgenesis and the abnormal shape of the internal capsule, we looked at whether specific mutation groups could be associated with absent, moderate (defined as hypoplastic, dysmorphic or hypogenetic) or severe (defined as partial or complete agenesis) corpus callosum abnormalities. The distribution of mutation type was similar in each group suggesting that we could not predict the degree of corpus callosum dysgenesis within a mutation group (data not shown). Moreover, among patients with recurrent mutations (i.e. p.R264C and p.R402H), we found a wide range of corpus callosum abnormalities (normal, hypogenesis or complete agenesis), suggesting that the mutation type could not help to determine the degree of alteration of corpus callosum development.

Finally, we attempted to evaluate whether mutation groups could correlate with the degree of cerebellar dysgenesis. Similar to the results obtained for corpus callosum dysgenesis, the distribution of mutation type did not differ among different groups (data not shown). Also, data for recurrent mutations indicate that the resulting cerebellar malformation is variable. For example, the mutation p.S172P was associated with normal cerebellum in one case and severe vermian dysplasia in the other. More interestingly, the mutation p.R264C resulted in either a normal, hypoplastic or severely dysgenetic cerebellum indicating that the mutation type could not help to determine the degree of cerebellar malformation.

Where biochemical and functional data were available, we compared our structure-based predictions to the actual ability of mutant tubulins to fold properly and assemble into microtubules, *in vitro* and in cells (Supplementary material). Remarkably, most mutants predicted to have an impaired folding (Group E) indeed showed a decreased ability to form heterodimers *in vitro*, although to variable extents. More surprisingly, several mutations whose

locations predicted primarily an alteration of interactions with microtubule-associated proteins were also found to alter heterodimer formation *in vitro*. In fact, these surface mutations might affect the stability of the protein, either directly by local perturbation of the structure, or indirectly through the interaction with chaperones or tubulin post-translational modification enzymes. In support, the discrepancies found between observations *in vitro* and in cells indicate that the consequences of mutations not only arise from the intrinsic properties of tubulin but also from its interaction with various cellular factors. In addition, as discussed previously regarding phenotypes, the biochemical properties of mutant tubulins are also differently altered depending on the precise nature of the substituted surface residue: e.g. TUBA1A R402C perturbs heterodimer formation much more dramatically than R402H. This emphasizes the limitations of predictions based on the structure of wild-type tubulin only, and therefore the need for a direct structural characterization of mutant tubulins, either on their own or in complex with relevant microtubule-associated proteins.

Conclusion

Through their structural role as building blocks of microtubules, tubulins play a large part in brain development; through neuronogenesis, neuronal migration, cortical organization–pial basement membrane integrity, and also in axon guidance through axonal leading process (growth cone) and maintenance. Therefore, for each tubulin isotype, the diversity of malformations might arise from the fact that different mutations may variably affect tubulin functions. Moreover, though recurrent mutations are consistently associated with almost identical cortical dysgeneses, at the current level of our understanding of tubulin functions and their cellular roles, predictions using structural data do not show definite correlation between the location of mutations and the degree of phenotype severity. Further structural characterization of tubulin mutants will be required to explain how the precise nature of a substitution can dramatically alter phenotype severity.

Acknowledgements

We would like to thank the patients and their families, as well as their referring physicians and genetic counsellors, without whom this study would not have been possible. We would like to thank Nathalie Carion, Magalie Percevault and Aurelie Toussaint for her help in performing molecular analysis. The authors are grateful to Dr M. Eiserman for their help in the analysis and the selection of EEG. We thank members of the Chelly lab for their thoughtful comments.

Funding

This work was supported by funding from INSERM, Fondation pour la Recherche Médicale (FRM; J Chelly—Equipe FRM 2013: DEQ2000326477), Fondation JED-Belgique, Agence National de Recherche (ANR Blanc 1103 01 - project R11039KK; ANR E-Rare-012-01 – project E10107KP), the EU-FP7 project GENECODYS, grant number 241995 and EU-FP7 project DESIRE, Grant agreement no: 602531.

Supplementary material

Supplementary material is available at *Brain* online.

References

Abdollahi MR, Morrison E, Sirey T, Molnar Z, Hayward BE, Carr IM, et al. Mutation of the variant alpha-tubulin TUBA8 results in polymicrogyria with optic nerve hypoplasia. Am J Hum Genet 2009; 85: 737–44.

Amrom D, Tanyalcin I, Verhelst H, Deconinck N, Brouhard G, Decarie JC, et al. Polymicrogyria with dysmorphic basal ganglia? Think tubulin! Clin Genet 2014; 85: 178–83.

Bahi-Buisson N, Poirier K, Boddaert N, Saillour Y, Castelnau L, Philip N, et al. Refinement of cortical dysgeneses spectrum associated with TUBA1A mutations. J Med Genet 2008; 45: 647–53.

Barkovich AJ. Current concepts of polymicrogyria. Neuroradiology 2010; 52: 479–87.

Barkovich AJ, Guerrini R, Kuzniecky RI, Jackson GD, Dobyns WB. A developmental and genetic classification for malformations of cortical development: update 2012. Brain 2012; 135 (Pt. 5): 1348–69.

Barkovich AJ, Hevner R, Guerrini R. Syndromes of bilateral symmetrical polymicrogyria. AJNR Am J Neuroradiol 1999; 20: 1814–21.

Barkovich AJ, Kuzniecky RI, Jackson GD, Guerrini R, Dobyns WB. A developmental and genetic classification for malformations of cortical development. Neurology 2005; 65: 1873–87.

Barkovich J. Complication begets clarification in classification. Brain 2013; 136 (Pt 2): 368–73.

Bilguvar K, Ozturk AK, Louvi A, Kwan KY, Choi M, Tatli B, et al. Whole-exome sequencing identifies recessive WDR62 mutations in severe brain malformations. Nature 2010; 467: 207–10.

Breuss M, Heng JI, Poirier K, Tian G, Jaglin XH, Qu Z, et al. Mutations in the beta-Tubulin Gene TUBB5 cause microcephaly with structural brain abnormalities. Cell Rep 2012; 2: 1554–62.

Cederquist GY, Luchniak A, Tischfield MA, Peeva M, Song Y, Menezes MP, et al. An inherited TUBB2B mutation alters a kinesin-binding site and causes polymicrogyria, CFEOM and axon dysinnervation. Hum Mol Genet 2012; 21: 5484–99.

Chew S, Balasubramanian R, Chan WM, Kang PB, Andrews C, Webb BD, et al. A novel syndrome caused by the E410K amino acid substitution in the neuronal beta-tubulin isotype 3. Brain 2013; 136 (Pt 2): 522–35.

Cushion TD, Dobyns WB, Mullins JG, Stoodley N, Chung SK, Fry AE, et al. Overlapping cortical malformations and mutations in TUBB2B and TUBA1A. Brain 2013; 136 (Pt 2): 536–48.

Dobyns WB, Truwit CL, Ross ME, Matsumoto N, Pilz DT, Ledbetter DH, et al. Differences in the gyral pattern distinguish chromosome 17-linked and X-linked lissencephaly. Neurology 1999; 53: 270–7.

Fallet-Bianco C, Loeuillet L, Poirier K, Loget P, Chapon F, Pasquier L, et al. Neuropathological phenotype of a distinct form of lissencephaly associated with mutations in TUBA1A. Brain 2008; 131 (Pt 9): 2304–20.

Guerrini R, Mei D, Cordelli DM, Pucatti D, Franzoni E, Parrini E. Symmetric polymicrogyria and pachygyria associated with TUBB2B gene mutations. Eur J Hum Genet 2012; 20: 995–8.

Higginbotham HR, Gleeson JG. The centrosome in neuronal development. Trends Neurosci 2007; 30: 276–83.

Hikita N, Hattori H, Kato M, Sakuma S, Morotomi Y, Ishida H, et al. A case of TUBA1A mutation presenting with lissencephaly and Hirschsprung disease. Brain Dev 2014; 36: 159–62.
Hoogenraad CC, Bradke F. Control of neuronal polarity and plasticity—a renaissance for microtubules? Trends Cell Biol 2009; 19: 669–76.
Jaglin XH, Chelly J. Tubulin-related cortical dysgeneses: microtubule dysfunction underlying neuronal migration defects. Trends Genet 2009; 25: 555–66.
Jaglin XH, Poirier K, Saillour Y, Buhler E, Tian G, Bahi-Buisson N, et al. Mutations in the beta-tubulin gene TUBB2B result in asymmetrical polymicrogyria. Nat Genet 2009; 41: 746–52.
Jansen AC, Oostra A, Desprechins B, De Vlaeminck Y, Verhelst H, Regal L, et al. TUBA1A mutations: from isolated lissencephaly to familial polymicrogyria. Neurology 2011; 76: 988–92.
Joshi HC, Cleveland DW. Diversity among tubulin subunits: toward what functional end? Cell Motility Cytoskeleton 1990; 16: 159–63.
Keays DA, Tian G, Poirier K, Huang GJ, Siebold C, Cleak J, et al. Mutations in alpha-tubulin cause abnormal neuronal migration in mice and lissencephaly in humans. Cell 2007; 128: 45–57.
Kumar RA, Pilz DT, Babatz TD, Cushion TD, Harvey K, Topf M, et al. TUBA1A mutations cause wide spectrum lissencephaly (smooth brain) and suggest that multiple neuronal migration pathways converge on alpha tubulins. Hum Mol Genet 2010; 19: 2817–27.
Lecourtois M, Poirier K, Friocourt G, Jaglin X, Goldenberg A, Saugier-Veber P, et al. Human lissencephaly with cerebellar hypoplasia due to mutations in TUBA1A: expansion of the foetal neuropathological phenotype. Acta Neuropathol 2010; 119: 779–89.
Leventer RJ, Jansen A, Pilz DT, Stoodley N, Marini C, Dubeau F, et al. Clinical and imaging heterogeneity of polymicrogyria: a study of 328 patients. Brain 2010; 133 (Pt 5): 1415–27.
Lopata MA, Cleveland DW. *In vivo* microtubules are copolymers of available beta-tubulin isotypes: localization of each of six vertebrate beta-tubulin isotypes using polyclonal antibodies elicited by synthetic peptide antigens. J Cell Biol 1987; 105: 1707–20.
Lowe J, Li H, Downing KH, Nogales E. Refined structure of alpha beta-tubulin at 3.5 A resolution. J Mol Biol 2001; 313: 1045–57.
Luduena RF. Are tubulin isotypes functionally significant. Mol Biol Cell 1993; 4: 445–57.
Mokanszki A, Korhegyi I, Szabo N, Bereg E, Gergev G, Balogh E, et al. Lissencephaly and band heterotopia: LIS1, TUBA1A, and DCX mutations in Hungary. J Child Neurol 2012; 27: 1534–40.
Morris-Rosendahl DJ, Najm J, Lachmeijer AM, Sztriha L, Martins M, Kuechler A, et al. Refining the phenotype of alpha-1a Tubulin (TUBA1A) mutation in patients with classical lissencephaly. Clin Genet 2008; 74: 425–33.
Nogales E, Wolf SG, Downing KH. Structure of the alpha beta tubulin dimer by electron crystallography. Nature 1998; 391: 199–203.
Norman MG, Roberts M, Sirois J, Tremblay LJ. Lissencephaly. Can J Neurol Sci 1976; 3: 39–46.
Okumura A, Hayashi M, Tsurui H, Yamakawa Y, Abe S, Kudo T, et al. Lissencephaly with marked ventricular dilation, agenesis of corpus callosum, and cerebellar hypoplasia caused by TUBA1A mutation. Brain Dev 2013; 35: 274–9.
Poirier K, Keays DA, Francis F, Saillour Y, Bahi N, Manouvrier S, et al. Large spectrum of lissencephaly and pachygyria phenotypes resulting from de novo missense mutations in tubulin alpha 1A (TUBA1A). Hum Mutat 2007; 28: 1055–64.
Poirier K, Lebrun N, Broix L, Tian G, Saillour Y, Boscheron C, et al. Mutations in TUBG1, DYNC1H1, KIF5C and KIF2A cause malformations of cortical development and microcephaly. Nat Genet 2013a; 45: 639–47.
Poirier K, Saillour Y, Bahi-Buisson N, Jaglin XH, Fallet-Bianco C, Nabbout R, et al. Mutations in the neuronal ss-tubulin subunit TUBB3 result in malformation of cortical development and neuronal migration defects. Hum Mol Genet 2010; 19: 4462–73.
Poirier K, Saillour Y, Fourniol F, Francis F, Souville I, Valence S, et al. Expanding the spectrum of TUBA1A-related cortical dysgenesis to Polymicrogyria. Eur J Hum Genet 2013b; 21: 381–5.
Romaniello R, Tonelli A, Arrigoni F, Baschirotto C, Triulzi F, Bresolin N, et al. A novel mutation in the beta-tubulin gene TUBB2B associated with complex malformation of cortical development and deficits in axonal guidance. Dev Med Child Neurol 2012; 54: 765–9.
Ross ME, Swanson K, Dobyns WB. Lissencephaly with cerebellar hypoplasia (LCH): a heterogeneous group of cortical malformations. Neuropediatrics 2001; 32: 256–63.
Sohal AP, Montgomery T, Mitra D, Ramesh V. TUBA1A mutation-associated lissencephaly: case report and review of the literature. Pediatric Neurol 2012; 46: 127–31.
Takanashi J, Barkovich AJ. The changing MR imaging appearance of polymicrogyria: a consequence of myelination. AJNR Am J Neuroradiol 2003; 24: 788–93.
Tischfield MA, Baris HN, Wu C, Rudolph G, Van Maldergem L, He W, et al. Human TUBB3 mutations perturb microtubule dynamics, kinesin interactions, and axon guidance. Cell 2010; 140: 74–87.
Tischfield MA, Cederquist GY, Gupta ML Jr, Engle EC. Phenotypic spectrum of the tubulin-related disorders and functional implications of disease-causing mutations. Curr Opin Genet Dev 2011; 21: 286–94.
Zanni G, Colafati GS, Barresi S, Randisi F, Talamanca LF, Genovese E, et al. Description of a novel TUBA1A mutation in Arg-390 associated with asymmetrical polymicrogyria and mid-hindbrain dysgenesis. Eur J Paediatric Neurol 2013; 17: 361–5.

Appendix 1

LIS-Tubulinopathies consortium: Jeanne Amiel, Marie-Claude Addor, Edith Andrini, Tania Attie-Bitach, Magalie Barth, Sophie Blesson, Lydie Burglen, Sebastien Cabasson, Claude Cances, Francoise Chapon, Aurore Curie, Alexandre Datta, Isabelle Desguerre, Patricia Dias, Bérénice Doray, Antoinette Gelot, David Genevieve, Brigitte Gilbert-Dussardier, Fabien Guimiot, Benedicte Héron, Delphine Héron, Marie Line Jacquemont, Frédérique Jossic, Pierre Simon Jouk, Annie Laquerrière, Sebastien Lebon, Jean Marie Lepage, Benoit Lhermitte, Philippe Loget, Laurence Loeuillet, Pascale Marcorelles, Mathieu Milh, Marie-Laure Moutard, Philippe Parent, Sandrine Passemard, Lucile Pinson, Chloé Quelin, Vincent des Portes, Ferechté Razavi, Nicole Revencu, Marlene Rio, Francois Rivier, Caroline Rouleau, Joelle Roume, Marc Tardieu.